MICROWAVE SYNTHESIS OF VANADIUM BASED OXIDE CATALYSTS

TEE CHEE KEONG

A project report submitted in partial fulfilment of the requirements for the award of Bachelor of Engineering (Hons.) Chemical Engineering

Faculty of Engineering and Science
Universiti Tunku Abdul Rahman

September 2011

DECLARATION

I hereby declare that this project report is based on my original work except for citations and quotations which have been duly acknowledged. I also declare that it has not been previously and concurrently submitted for any other degree or award at UTAR or other institutions.

Signature : _____

Name : _____

ID No. : _____

Date : _____

APPROVAL FOR SUBMISSION

I certify that this project report entitled **"MICROWAVE SYNTHESIS OF VANADIUM BASED OXIDE CATALYSTS"** was prepared by **TEE CHEE KEONG** has met the required standard for submission in partial fulfilment of the requirements for the award of Bachelor of Engineering (Hons.) Chemical Engineering at Universiti Tunku Abdul Rahman.

Approved by,

Signature : _____

Supervisor : Dr. Leong Loong Kong

Date : _____

Specially dedicated to
my beloved mother and father

ACKNOWLEDGEMENTS

I would like to express my gratitude to my research supervisor, Dr. Leong Loong Kong for his invaluable advice, guidance and his enormous patience throughout the development of the research.

Besides, I would like to thank my seniors, Miss Zoey Kang and Mr. Matthew Wong for their valuable helps on my research.

In addition, I would also like to express my gratitude to my loving parents, loved one and friends who had helped and given me encouragement and support. Lastly, I would like to thank everyone who had contributed to the successful completion of this project.

MICROWAVE SYNTHESIS OF VANADIUM BASED OXIDE CATALYSTS

ABSTRACT

Vanadium phosphorus oxide (VPO) catalysts were prepared via sesquihydrate precursor ($VOHPO_4 \cdot 1.5H_2O$) method by microwave treatment method using microwave digester. The first stage microwave treatment was set to be constantly 1 hour and second stage microwave treatment of 4, 5, 6 and 7 hours. Normal drying method was applied to dry the precursors produced for both stages. The precursors produced were calcined in a reaction air flow of 0.75 % *n*-butane in air for 18 hours. The catalysts synthesised were denoted as VPO-4, VPO-5, VPO-6 and VPO-7. The effects of different second stage microwave treatment durations towards the physical and chemical properties of VPO catalysts were studied. The results showed that VPO-6 has the least formation of V^{5+} phase as seen in XRD patterns at 2θ = 28.4 ° and exhibited the highest specific surface area of 17.049 m^2/g as seen in BET analysis. Microwave treatment duration more or less than 6 hours led to the increased in formation of V^{5+} phase and decreased of specific surface area. However, different microwave treatment durations did not show much different on the crystalline sizes and rosette-shape morphologies of all catalysts synthesised. The P/V ratio obtained from both EDX and ICP-OES were less than one, showing that the microwave treatment would reduce the phosphorus (P) contents of the catalysts. VPO-6 has the highest P/V ratio (0.95) and closest to 1. Generally, the increase of second stage microwave treatment durations had decreased the average oxidation number of vanadium (V_{AV}) as seen in redox titration. However, the V_{AV} value increased again if the microwave treatment duration was too long. This is due to the presence of more V^{5+} phase, which was observed in the XRD patterns.

TABLE OF CONTENTS

LIST OF TABLES

LIST OF FIGURES

LIST OF SYMBOLS / ABBREVIATIONS

c_p	specific heat capacity, J/(kg·K)
S	selectivity of the desired product, %
t	crystallite size for (*h k l*) phase, Å
V_1	volume of potassium permanganate used in first stage, cm^3
V_2	volume of ammonium iron (II) sulphate used in second stage, cm^3
V_3	volume of ammonium iron (II) sulphate used in third stage, cm^3
V^{3+}	concentration of vanadium at oxidation number of +3
V^{4+}	concentration of vanadium at oxidation number of +4
V^{5+}	concentration of vanadium at oxidation number of +5
V_{AV}	average oxidation number of vanadium (V_{AV})
β_{hkl}	full width at half maximum (FWHM) at (*h k l*) peak, rad
θ_{hkl}	diffraction angle for (*h k l*) phase, °
λ	X-rays wavelength of radiation for Cu Kα, Å
VPO	vanadium phosphorus oxide
V^{3+}	vanadium at oxidation state of +3
V^{4+}	vanadium at oxidation state of +4
V^{5+}	vanadium at oxidation state of +5

LIST OF APPENDICES

CHAPTER 1

INTRODUCTION

1.1 Catalyst and Catalysis

Catalyst is defined as a substance that affects the rate of chemical reaction without being consumed itself, and without altering the equilibrium constant of the reaction. It mainly provides a different molecular pathway with a lower energy barrier, affecting both the selectivity and yield (Fogler, 2006). As seen in Figure 1.1, the dotted line represents a catalysed chemical reaction shows lower activation required for the same process if compared to reaction without catalyst. A catalyst accelerates a chemical reaction by forming bonds with the reacting molecules, allowing these to react to a product, which detaches from the catalyst, and leaves it unaltered such that it is available for the next time (Chorkendorff & Niemantsverdriet, 2003).

Catalysis is a term coined by Baron J. J. Berzelius in 1835 to describe the property of substances that facilitate chemical reactions without being consumed in term. Fogler (2006) stated that catalysis is the occurrence, study and use of catalyst and catalytic processes.

Figure 1.1 shows a catalytic reaction between two molecules A and B to give a product P. The reaction starts with the bonding of molecules A and B to the catalyst. Molecules A and B then have reaction within this complex to give a molecule of product P, which is also bound to the catalyst. Lastly, product P separates from the catalyst, leaving the catalyst to be reused. The figure also compares the non-catalytic reaction path with the catalytic reaction path. Obviously, the catalyst offers an

alternative path for the reaction with significantly lower activation energy. The catalyst does not affect the equilibrium constant for the overall reaction of A + B to P.

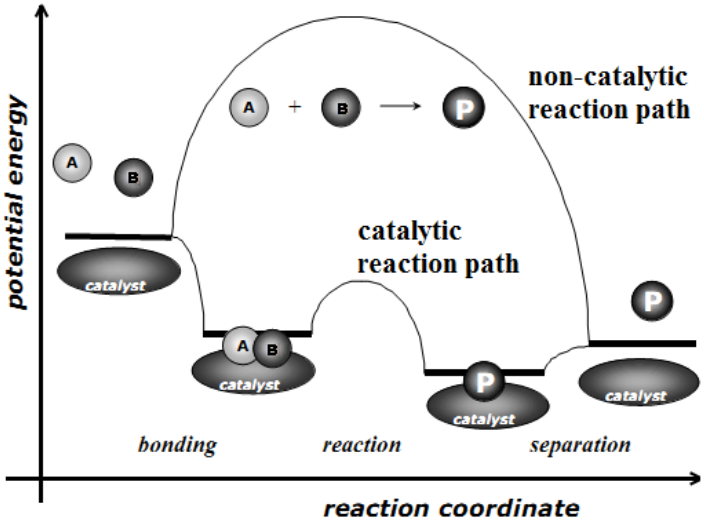

Figure 1.1: Simple Mechanism of Heterogeneous Catalytic Reaction

1.1.1 Types of Catalysis

There are three types of catalysis, homogeneous catalysis, heterogeneous catalysis and biocatalysis. The classification between homogeneous and heterogeneous catalysis depends on the whether a catalyst is in the same phase as the reactant. Biocatalysis used enzyme as the nature's catalysts to speed up the reaction (Chorkendorff & Niemantsverdriet, 2003).

1.1.1.1 Homogeneous Catalysis

Homogeneous catalysis concerns processes in which a catalyst is in the same phase (usually liquid phase) with at least one of the reactants (Fogler, 2006). Homogeneous catalysts have the advantage of being totally reproducible because of their definite stoichiometry and structure. The major disadvantage of homogeneous catalysts is the

problem of separating the expensive catalyst from the products at the end of the reaction since they are in the same phase. A very efficient distillation or ion-exchange process is required (Hartley, 1985). Besides, homogeneous catalysts have only one type of active side and therefore they will often be more specific than heterogeneous catalysts.

An example of homogeneous catalysis is the industrial Oxo process. It has propylene, carbon monoxide and hydrogen as the reactants and a liquid-phase cobalt complex as the catalyst.

1.1.1.2 Heterogeneous Catalysis

A heterogeneous catalytic process involves more than one phase where the phase of the catalyst differs from that of the reactants. Majority of heterogeneous catalysts are solids and reactants are gases or liquids (Rothenberg, 2008). An example of heterogeneous catalysis is the VPO catalyst studied in this research. The VPO catalyst is in solid phase and *n*-butane is in gaseous phase.

Fogler (2006) has proposed that there are seven steps in a heterogeneous catalytic reaction, which are:

1. External diffusion of the reactant from the bulk fluid to the external surface of the catalyst pellet.
2. Internal diffusion of the reactant from the pore mouth through the catalyst pores to the internal catalytic surface.
3. Adsorption of the reactant onto the catalyst surface
4. Reaction on the surface of the catalyst.
5. Desorption of the product from the catalyst surface
6. Internal diffusion of the product from the internal catalytic surface through the catalyst pores to the pore mouth.
7. External diffusion of the product from the external surface of the catalyst pellet to the bulk fluid.

To the seven steps in a catalytic reaction stated above, the most important are step 3, 4 and 5, which are the adsorption of reactant, reaction of reactant to product and the desorption of product. After desorption process, the catalysts can be separated from the product easily, and the catalysts can be reused. This simple mechanism is shown in Figure 1.2 below:

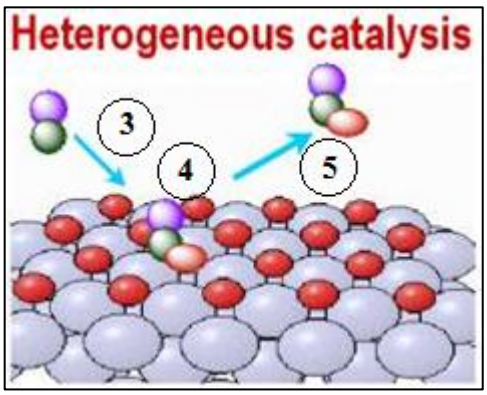

Figure 1.2: Simple Mechanism of Heterogeneous Catalytic Reaction

Heterogeneous catalysts have the major advantage of simple separation of catalysts from the product, which can be achieved by some kind of filtration. However, in a heterogeneous catalytic system, the catalytic reaction must necessarily take place on the surface of the catalyst so that there are parts of the catalyst not present at the surface remain unused (Hartley, 1985). Therefore, a heterogeneous catalytic reaction is higher dependant on the surface area of the catalyst.

1.1.1.3 Biocatalysis

Biocatalysis is the catalytic reaction that uses enzyme as the catalyst to speed up the reaction. Enzymes are nature's catalysts with very shape-specific active sites, which make them to be highly specific and efficient catalysts (Chorkendorff & Niemantsverdriet, 2003). However, enzymes are neither homogeneous nor heterogeneous and not related to this research.

1.1.2 Properties of Good Catalysts

Hartley (1985) has proposed that a commercially usedful catalyst must posses three major desirable features, which are activity, selectivity and life span. These 3 features determine the performance of the catalyst.

Activity is defined as the rate at which a chemical reaction reaches equilibrium (David & Sharp, 2003). The activity of catalyst is also known as the conversion of the reactant, which is the percentage of reactant that reacted. Higher activity of the catalyst means more reactants are converted into product or by-product, or in other words less reactants remained after the reaction. It can be represented by the equation below:

$$Conversion\ of\ Reactant\ A = \frac{Moles\ of\ A\ reacted}{Moles\ of\ A\ fed\ in} \times 100\% \qquad (1.1)$$

Selectivity is defined as the ratio of amount of desired product to the amount of undesired products. Most of the real life reaction involving multiple reaction, selectivity tells how one product is favoured over another (Fogler, 2006). Selectivity is defined by the equation below:

$$S = \frac{Moles\ of\ Desired\ Product}{Moles\ of\ Undersired\ Product} \times 100\% \qquad (1.2)$$

where

S = selectivity of the desired product, %

High selectivity indicates the final product is mostly the desired one, less by-product in final. Therefore, catalyst must exhibit high selectivity not only to have more desired product, but also to reduce the cost of separating the desired products from the by-products (Hartley, 1985).

Life Span is defined as the period of time required for the efficiency of the catalyst to be dropped to the unacceptable level. After that time, the catalyst needed to be replaced to have good reaction. This is important to the expensive catalyst, which requires high cost of exchanging.

1.1.3 Applications of Catalysts

Catalysts accelerate reactions and enable industrially reactions to be carried out more efficiently. Catalytic routes can be designed to utilise the use of raw materials and reduce waste production. Therefore, about 85-90 % of all products in chemical industry are made in catalytic processes (Chorkendorff & Niemantsverdriet, 2003). The development and use of catalysis is a major part of the constant search for new ways of increasing product yield and selectivity from chemical reactions (Fogler, 2006). Nowadays, catalysts are used in most of the manufacturing process, for the fields of petrochemical, fine chemistry and pharmaceutical (Ertl & Freund, 1999).

In the 1920's petroleum-processing was limited to rectification and decomposition by heating to high temperature without catalyst. Only in late 30's were the first attempts to apply catalytic processes in petroleum-processing. The efficiency of catalysis applied led to a sharp increase of both the yield and the quality. At present, more than 80 % of oil is processed through catalytic cracking, reforming, hydrocracking and others (Boreskov, 2003).

1.2 Selective Oxidation

Oxidation is a chemical combination of a substance with oxygen. Centi, Cavani, & Trifiro (2001) summaried 4 important limitations in catalytic oxidation:

1. None of the reactions runs at maximum selectivity due to the formation of undesired by-products.
2. Processes can generate co-products that are not always of economic interest.
3. Some raw materials and products are suspected or proven carcinogens.
4. Some processes require expensive oxidising agents.

Oxidation reactions play an important role in both the science of catalysis and catalysis-based modern chemical industry (Ruiz & Delmon, 1992). Therefore, catalyst is required to make the oxidation process to be selectively to produce the desired product. Selective oxidation of hydrocarbons is particularly challenging for chemical engineers because the final result depends on some opposing factors:

1. In hydrocarbon oxidation processes thermodynamics favours the ultimate formation of carbon dioxide and water, therfore all products of partial oxidation are derived by kinetic control of the reaction
2. All oxidation processes are strongly exothermic and efficient heat removal must be secured to control the temperature and prevent over-oxidation as well catalyst damage.

An example of selective oxidation is the oxidation of *n*-butane in this research. The oxidation of *n*-butane leads to 3 different products, which are acetic acid, acetaldehyde and maleic anhydride (Matar & Hatch, 2000). With the help of VPO catalyst, the oxidation of *n*-butane becomes selectively oxidised to produce maleic anhydride.

1.3 Problem Statement

At present, more than 70% of maleic anhydride is produced from *n*-butane oxidation. However, the productivity from *n*-butane is still considered low due to its low selectivity and conversion (Kroschwitz & Howe-Grant, 1991). Under typical industrial conditions (2 mol. % *n*-butane in air, 673-723 K, and space velocities of 1100-2600 h^{-1}), the selectivity of maleic anhydride for fixed-bed reactor is only 67-75 mol. % with *n*-butane conversion of 70-85 %. It is still desirable to invest in improving catalyst performance as profit margins can be increased by improving the selectivity or activity of the process (Centi, Cavani, & Trifiro, 2001).

The intermediates of the selective oxidation of *n*-butane to maleic anhydride have been determined by several authors, but there is little information on the intermediates adsorbed on the catalyst surface. A better catalysis system can be developed if the interaction of the reactants with the catalytic surface can be understood (Ramstetter & Baerns, 1988).

1.4 Objectives

1. To synthesise the VPO catalysts through microwave treatment and normal oven drying.
2. To study the effect of different second stage microwave treatment durations towards the physical and chemical properties of VPO catalysts.

CHAPTER 2

LITERATURE REVIEW

2.1 Vanadium Phosphorus Oxide (VPO) Catalyst

VPO is known as catalysts for the selective oxidation of *n*-butane to maleic anhydride. Many efforts have been done to improve its activity and selectivity. However, the oxidation mechanism has not yet been fully understood, and the nature of the active sites is still being discussed (Bergeret, David, Broyer, & Volta, 1987).

VPO catalyst is a fascination and complex catalytic system. There are various distinct compounds cane be formed: α-, β-, γ-$VOPO_4$, $VOHPO_4{\cdot}4H_2O$, $VOHPO_4{\cdot}0.5H_2O$, $VO(H_2PO_4)_2$, $VO(PO_3)_2$ and β-, γ- $(VO)_2P_2O_7$ (Centi, 1993). VPO catalyst consists of 3 different phases with vanadium in oxidation states of +3 +4 and +5. The V^{3+} phases correspond to VPO_4 and $V(PO_3)_3$. The V^{4+} phases correspond to $VOHPO_4{\cdot}0.5H_2O$, $(VO)_2P_2O_7$ and $VO(PO_3)_2$. Lastly, the V^{5+} phases correspond to $VOPO_4{\cdot}H_2O$ and $VOPO_4$ (Abon & Volta, 1997).

Different oxidation state of vanadium can be classified by their colour. Yellow colour for VO_2^+ (+5 oxidation state), on reduction VO_2^+ transform into blue VO^{2+} (+4 oxidation state), and lastly reduced again to green V^{3+} (Haber, 2009). The summary of corresponding VPO compounds and colour of different vanadium phases were shown in Table 2.1.

Table 2.1: Summary of Different Vanadium Phases

Phases	Corresponding Compounds	Colour
V3+	VPO_4 $V(PO_3)_3$	Yellow
V4+	$VOHPO_4 \cdot 0.5H_2O$ $(VO)_2P_2O_7$ $VO(PO_3)_2$	Blue
V5+	$VOPO_4 \cdot H_2O$ $VOPO_4$	Green

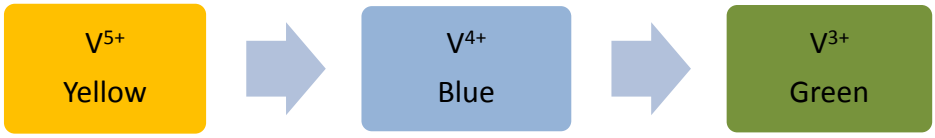

Figure 2.1: Colour of Vanadium at Different Oxidation State

Vanadyl pyrophosphate, $(VO)_2P_2O_7$ is considered to be the active and selective crystalline phase of the *n*-butane oxidation to maleic anhydride (Bordes & Courtine, 1979). This is a structure in which two octahedral are joined by edges. Octahedral pairs are connected by PO_4 tetrahedral which gives a layer structure in the (001) plane. The idealised structure of this $(VO)_2P_2O_7$ is shown in Figure 2.1 below. The vanadium lies on the plane, the phosphorus and oxygen attach on the both sides of the vanadium plane.

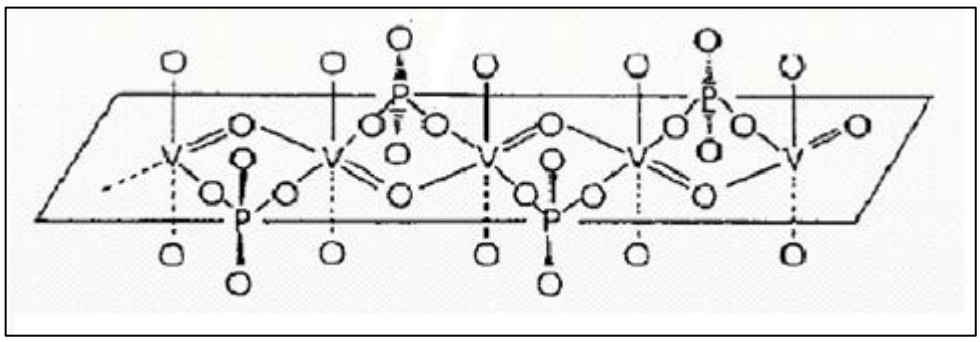

Figure 2.2: Idealised Structure of $(VO)_2P_2O_7$

2.2 Synthesis Routes to VPO Catalyst

There are few ways to produce VPO catalyst, by which the physicochemical properties and the catalytic performances are strongly depends on the preparation methods. Generally, VPO catalysts are produced through vanadium oxide (V_2O_5) and phosphoric acid (H_3PO_4) as the vanadium and phosphorus sources respectively.

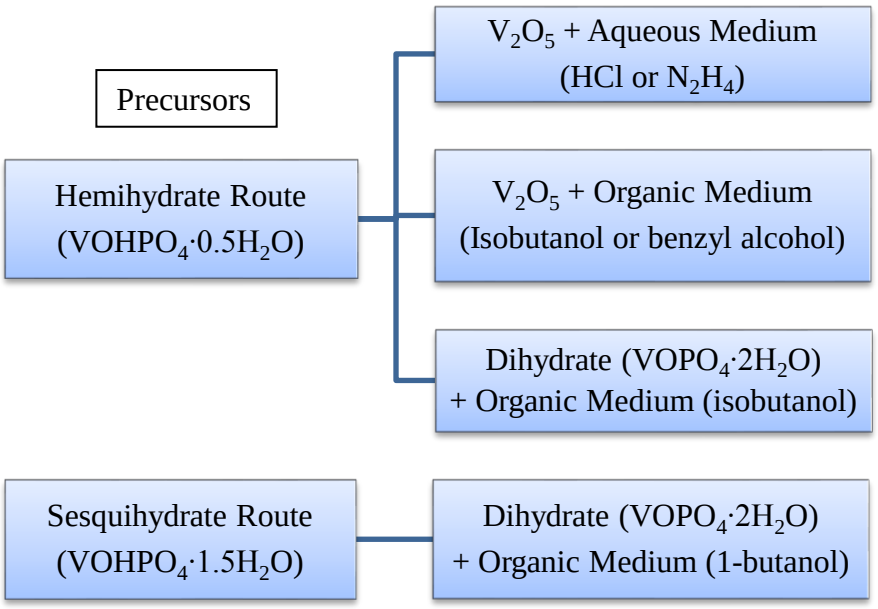

Figure 2.3: Synthesis Routes towards VPO Catalysts

Figure 2.3 shows that there are 2 different precursors routes lead to the production of VPO catalyst, which are vanadyl phosphohemihydrate ($VOHPO_4 \cdot 0.5H_2O$) and vanadyl hydrogenphosphate sesquihydrate ($VOHPO_4 \cdot 1.5H_2O$). 3 different methods are available for hemihydrate precursor and 1 method for sesquihydrate precursor. Both of the precursors produced require undergoing calcination to activate them to VPO catalyst. Different methods of preparation will produce VPO catalyst with different specific area, but not affecting the nature of active sites (Shima & Hatano, 1997).

2.2.1 Hemihydrate Precursor Route ($VOHPO_4 \cdot 0.5H_2O$)

There are 3 different routes to produce hemihydrate precursor, which are aqueous medium route, organic medium route and through dihydrate route.

In aqueous medium, V_2O_5 is reduced by a mineral agent such as hydrochloric acid (HCl) and hydrazine (N_2H_4) in water and H_3PO_4. The main precursor compound prepared is the vanadyl phosphohemihydrate, $VOHPO_4 \cdot 0.5H_2O$ (V^{4+}) and require calcination to produce VPO catalyst. The VPO catalyst produced via aqueous medium has a poor performance for *n*-butane oxidation due to its low surface area and therefore the catalyst activity is low (Abon & Volta, 1997).

In organic medium, V_2O_5 is reduced by an organic reagent like methanol (CH_3OH), isobutanol ($C_4H_{10}O$) or benzyl alcohol (C_7H_8O) prior to the addition of phosphoric acid (Abon & Volta, 1997). The main precursor compound prepared is the vanadyl phosphohemihydrate, $VOHPO_4 \cdot 0.5H_2O$ (V^{4+}) and require calcination to produce VPO catalyst. VPO catalyst produced via organic medium has higher specific surface area and greater density of active sites, so it tends to have higher reactivity (Cavani & Trifiro, 1994).

The third route is to reduce vanadium phosphate dihydrate ($VOPO_4 \cdot 2H_2O$) in organic medium. V_2O_5 is mixed with H_3PO_4 and water to produce dihydrate first, and then the dried dihydrate is reduced in organic medium like isobutanol. The main precursor produced will be vanadyl phosphohemihydrate, $VOHPO_4 \cdot 0.5H_2O$ (V^{4+}) and require calcination to produce VPO catalyst. The final precursor from dihydrate route gives a higher specific surface area as compared to the aqueous medium route (Abon & Volta, 1997).

2.2.2 Sesquihydrate Precursor Route ($VOHPO_4 \cdot 1.5H_2O$)

There is only one way to produce vanadium hydrogen phosphate sesquihydrate ($VOHPO_4 \cdot 1.5H_2O$) precursor. This method is similar to the dihydrate route to produce hemihydrate precursor. V_2O_5 is mixed with H_3PO_4 and water to produce dihydrate ($VOPO_4 \cdot 2H_2O$) first, and then the dried dihydrate is reduced in *1*-butanol. The dihydrate will be reduced to vanadium hydrogen phosphate sesquihydrate ($VOHPO_4 \cdot 1.5H_2O$) precursor (Ishimura, Sugiyama, & Hayashi, 2000). After calcination, the VPO catalyst produced via sesquihydrate route gave high specific activity in selective oxidation of *n*-butane to maleic anhydride (Taufiq-Yap, Leong, Hussien, Irmawati, & Hamid, 2004). Sesquihydrate precursor route with microwave treatment is the method used to produce VPO catalysts in this research.

2.3 Factors Affecting the Performance of VPO Catalyst

As discussed in section 2.2, the performance and characteristic of VPO catalyst are strongly depends on the synthesis route of its precursor. Centi et al. (1988) had reported that there are few other factors affecting the performance of VPO catalyst, which are:

1. Precursor routes
2. Calcination conditions
3. P/V ratio
4. Support system
5. Addition of promoter
6. Microwave treatment duration

The effects of four different precursor routes towards VPO catalysts were discussed in section 2.2.

2.3.1 Calcination Conditions

In this research, calcination is used to convert the VPO precursor into active VPO catalyst through an *n*-butane air treatment at high temperature. The duration, temperature and the atmosphere (composition of air) are affecting the structure, performance of the active VPO catalyst (Taufiq-Yap et al., 2001).

Increasing the duration of reaction with *n*-butane/air mixture led to an increase in the total surface area. It also led to the complete removal of the $VOPO_4$ phase from the VPO catalysts. A longer periods of pre-treatment in the *n*-butane/air mixture produced VPO catalysts with increasing amount of rosette-type of agglomerate (Taufiq-Yap et al., 2001).

Sadiq et al. (2011) had studied the effect of different calcination temperature to the activity of the VPO catalyst. They found that the catalyst calcined at 723 K (450 ℃) exhibits catalytic activity higher than that calcined at 973 K (700 ℃). However, the selectivity of isopropanol towards propene is higher for the catalyst calcined at 973 K.

Different calcination atmosphere affects the catalyst morphology and the vanadium valence (Wang & Wang, 1997). The catalyst calcined in *n*-butane/air gave higher surface area compared to the catalyst calcined in propane/air. The amount of V^{5+} is also higher for the catalyst calcined in *n*-butane/air (Taufiq-Yap & Saw, 2008). However, the calcination durations for all VPO precursors were set to be constantly 18 hours in this research.

2.3.2 P/V Ratio

P/V ratio is the atomic ratio of phosphorus to vanadium in VPO catalyst. The P/V ratio strongly influences the final redox state obtained by VPO catalysts and the final catalytic properties (Bergeret, David, Broyer, & Volta, 1987).

The optimal catalyst composition is characterised by a slight excess of phosphate with respect to the empirical formula of the $VOHPO_4 \cdot 0.5H_2O$ precursor (Cornaglia, C.Caspani, & Lombardo, 1991). In catalysts with low phosphate concentration (low P/V ratio) leads to the oxidation of V^{4+} to V^{5+}, high phosphate concentration (high P/V ratio) causes low reducibility of V^{4+}. The increased of V^{5+} content leads to a higher activity but lower selectivity VPO catalyst. Therefore, VPO catalysts require only a slight excess of phosphate (P/V ratio = 1 to 1.2) to compromise between oxidisability and reducibility to obtain both high activity and selectivity in *n*-butane oxidation (Spivey, Guliants, & Carreon, 2005).

2.3.3 Support System

Small metal particles are often unstable and prone to sintering. Heterogeneous catalysts used in industry consist of relatively small particles stabilised in some way to against sintering. This can be achieved by adding a support system, so called structural promoter. All kinds of materials those are thermally stable and chemically relatively inert can be used as support. Alumina, silica and carbon are the most common, with magnesia, zinc oxide, silicon carbide and zeolites used for particular applications. (Chorkendorff & Niemantsverdriet, 2003).

Silica has been used as the support material for VPO catalysts in most studies. However, according to the research done by Kuo & Yang (1989), they found that aluminium phosphate ($AlPO_4$) is a better support material over silica for VPO catalysts. This is because $AlPO_4$ has a strong thermal stability suitable for highly exothermic reactions, (ii) large pore diameter to minimise degree of overreaction, and (iii) positive interaction between VPO and $AlPO_4$ to make the supported VPO more selective to maleic anhydride production.

2.3.4 Addition of Doping Agent (Dopant)

Dopant is a small amount of impurity element inserted into the lattice of VPO catalyst to affect the performance of the catalyst. VPO has been often doped with various metals to increase its surface area, alter the V^{4+}/V^{5+} ratio or the amount of energetic oxygen species at the surface. The promoting effect of doping ions was found to be either structural, electronic, or a combination of both (Delimitis, 2010). Various dopants such as cobalt (Co), molybdenum (Mo), chromium (Cr), iron (Fe), cerium (Ce), zinc (Zn), titanium (Ti), zirconium (Zr) and silicon (Si) have been added to VPO to improve its catalytic performance (Kamiya, Kijima, Ohkura, Satusuma, & Hattori, 2003). Examples of additional of dopant to VPO catalyst are discussed below:

The additional of cobalt (Co) dopant to VPO catalyst improves the yield of *n*-butane to maleic anhydride. Besides, the presence of cobalt phosphate stabilises the excess phosphorus present in VPO catalyst (Cornaglia, Irusta, Lombardo, Durupty, & Volta, 2003). Taufiq-Yap (2006) found that both chromium (Cr) and cobalt (Co) dopants improve strongly the *n*-butane conversion without sacrificing the maleic anhydride selectivity.

The incorporation of bismuth (Bi) into VPO catalysts lattice increased the surface area and lowered the overall vanadium oxidation state. The addition of Bi also increased the total amount of oxygen removed from the catalysts. Bi-doped VPO catalysts were found to be highly active due to the catalysts possess highly active and labile lattice oxygen (Taufiq-Yap, Kamiya, & Tan, 2006).

For iron (Fe) doped VPO catalysts, the catalytic activity for maleic anhydride formation per unit surface area was higher than the undoped VPO catalysts. The doped Fe ions uniformly spread in the bulk of the VPO catalyst and were substituted for V^{4+} in the $(VO)_2P_2O_7$ crystal. The doped Fe ions can enhance the redox ability, resulting in the high catalytic performance (Kamiya, Kijima, Ohkura, Satusuma, & Hattori, 2003).

2.3.5 Duration of Microwave Treatment

Microwave treatment method was applied to prepare many catalysts such as Zn-ZSM-5-based catalysts (Janjic & Scurrell, 2002), alumina-supported palladium-iron bimetallic catalysts (Berry, Smart, Prasad, Lingaiah, & Rao, 2000). These catalysts showed better performance in the reaction of selective oxidation alkyl to olefin and other chemical feed.

However, microwave treatment is a newly developed and poorly understood method to produce VPO catalyst. Theoretically, durations of both stages of microwave treatment should affect the VPO catalysts in some distinct. Study of the effect of different second stage microwave treatment duration to the VPO catalysts is the objective of this research. In this research, second stage microwave treatments varied from 4, 5, 6 and 7 hours. The VPO catalysts synthesised were analysed by various methods to test their physical and chemical properties.

2.4 Maleic Anhydride

Maleic anhydride ($C_4H_2O_3$) has an IUPAC name of furan-2,5-dione. The structure of maleic anhydride is shown in Figure 2.4 below:

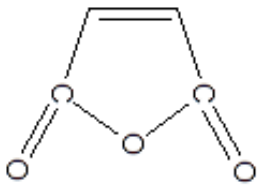

Figure 2.4: Structure of Maleic Anhydride

Maleic anhydride was first produced by dehydration of maleic acid. Nowadays, maleic anhydride can be produced through 3 oxidation routes: *n*-butane oxidation, *n*-butene oxidation and benzene oxidation (Matar & Hatch, 2000). C4 hydrocarbons (*n*-butane and *n*-butene) has been replacing benzene to produce maleic anhydride (Felthouse et al., 2001). This is due to the reasons below:

1. Benzene is not environmental friendly, it causes leukaemia.
2. Benzene (C_6H_6) has 6 carbons, which lose 2 carbons when oxidised to maleic anhydride ($C_4H_2O_3$) with only 4 carbons.
3. Benzene is more expensive and low availability

As comparing the two C4 hydrocarbons, *n*-butane and *n*-butene, *n*-butane is cheaper than *n*-butene and the selectivity to maleic anhydride from butene is lower than from butane (Busca, Centi, & Trifiro, 1987). Therefore, oxidation of *n*-butane is the main source for the production of maleic anhydride (Matar & Hatch, 2000). At present, more than 70 % of maleic anhydride is produced from *n*-butane oxidation (Kroschwitz & Howe-Grant, 1991).

Maleic anhydride is an important chemical which polymerises with other monomers while retaining the double bond, as in unsaturated polyester resins. The polyester resins produced are used primarily in fibre-reinforced plastics for the construction, marine and transportation industries (Matar & Hatch, 2000). In 1995, the global production of maleic anhydride had grown to an estimated 900,000 tons with a value of $700 million (Centi, Cavani, & Trifiro, 2001).

2.5 *n*-butane Oxidation to Maleic Anhydride

Bergman & Frisch (1966) disclosed that selective oxidation of *n*-butane was catalysed by the VPO catalysts. The catalyst used is the VPO catalyst, which provides the oxygen needed for the oxidation (Matar & Hatch, 2000). Oxidation process of *n*-butane is becoming a major source for maleic anhydride.

According to Matar & Hatch (2000), the selective oxidation of *n*-butane to maleic anhydride involves a redox mechanism of removing eight hydrogen atoms (reduction) as water and inserting of three oxygen atoms (oxidation) into the butane molecule. The overall reaction is simplified as the equation below:

$$C_4H_{10} + 7/2\ O_2 \xrightarrow[VPO]{} C_4H_2O_3 + 4H_2O$$

The reaction pathway actually involves the formation of maleic anhydride and by-products of carbon oxides from *n*-butane. The conversion of maleic anhydride to CO, CO_2 and H_2O and have postulated the oxidation of maleic anhydride on the basic of kinetic modelling (Moser, Wenig, & Schrader, 1987).

2.6 Microwave Treatment

Microwave treatment method was applied to prepare many catalysts such as Zn-ZSM-5-based catalysts (Janjic & Scurrell, 2002), alumina-supported palladium-iron bimetallic catalysts (Berry, Smart, Prasad, Lingaiah, & Rao, 2000). These catalysts showed better performance in the reaction of selective oxidation alkyl to olefin and other chemical feed.

However, using microwave irradiation to build up temperature of preparation process method is a newly and poorly understood method to produce VPO catalysts (Zeng, Jiang, & Niu, 2005). Traditionally, VPO precursor was produced from vanadium oxide (V_2O_5) through reflux method.

By comparing, the traditional method (reflux) takes about 1 day to produce vanadium phosphate dihydrate and another 1 day to produce vanadium hydrogen phosphate sesquihydrate precursor (Ishimura, Sugiyama, & Hayashi, 2000). For new method (microwave treatment) that used in this research, it took about 1 hour to produce dihydrate precursor, and another 4 to 7 hours to produce sesquihydrate precursor.

In this research, VPO catalyst was produced via sesquihydrate precursor route by microwave treatment method. The VPO catalyst synthesised was then characterised to study the effect of different microwave treatment durations towards its physicochemical properties.

CHAPTER 3

METHODOLOGY

3.1 Materials and Gases

The table below shows the chemicals and gases used throughout this project:

Table 3.1: Chemicals and Gases Used

No.	Materials	Formula	Company
1	Vanadium (V) pentoxide	V_2O_5	UNI Chem
2	*ortho*-Phosphoric acid	*o*-H_3PO_4 (85%)	Merck
3	1-Butanol	$CH_3(CH_2)_3OH$	R&M Chemicals
4	Potassium permanganate	$KMnO_4$	HmbG Chemicals
5	Nitric acid	HNO_3	R&M Chemicals
6	Sulphuric acid (95-98 %)	H_2SO_4	Systerm
7	Ammonium iron (II) sulphate	$(NH_4)_2Fe(SO_4)_2$	R&M Chemicals
8	0.75 % *n*-butane in air		Malaysia Oxygen Berhad (MOX)
9	99.99 % Purified nitrogen		Malaysia Oxygen Berhad (MOX)
10	99.99 % Purified helium		Malaysia Oxygen Berhad (MOX)

3.2 Preparation of VPO Catalyst

The preparation of VPO catalyst has been produced through the sesquihydrate precursor ($VOHPO_4 \cdot 1.5H_2O$) in this project. The production of the catalyst requires 3 stages: first stage of microwave treatment, second stage of microwave treatment and calcination of the catalyst. The VPO catalyst produced was then analysed by some characterisation techniques.

3.2.1 1st Stage of Microwave Treatment

(Refer to Figure 3.1: 1st Stage of Microwave Treatment)

Firstly, 2.5 g of vanadium oxide (V_2O_5) was inserted into one of the closed vessel. Then 60 ml of distilled water and *ortho*-phosphoric acid, *o*-H_3PO_4 (85%) were added to the vessel. The addition of V_2O_5, distilled water and *o*-H_3PO_4 was repeated to fill up all the 6 closed vessels. These 6 vessels were then treated by microwave irradiation (1450 W) at 120 ℃ for 1 hour in a microwave digester.

After 1 hour of microwave treatment and about 20 minutes of cooling, the vessels were removed from the microwave digester. A yellow solution with yellow solid suspension was formed. The yellow solid was then recovered using centrifuge technique and dried in oven for 48 hours. Dried yellow solid precursor of $VOPO_4 \cdot 2H_2O$ was obtained.

+

6 × $V_2O_5 + o\text{-}H_3PO_4 + H_2O$

Closed Vessels

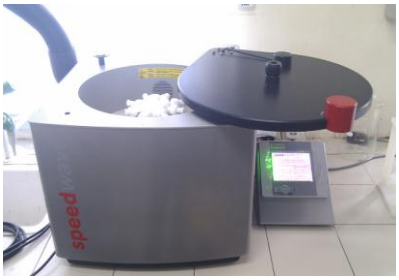

1st Stage Microwave Treatment (1450 W):
1 hour 120 °C

Yellow solid formed (wet)

Centrifugation

Normal Oven Drying:
48 hour 90 °C

1st Stage
$VOPO_4 \cdot 2H_2O$
Dry yellow solid

Figure 3.1: 1st Stage of Microwave Treatment

3.2.2 2nd Stage of Microwave Treatment

(Refer to Figure 3.2: 2nd Stage of Microwave Treatment)

Firstly, 2.5 g of dried yellow solid ($VOPO_4 \cdot 2H_2O$) obtained from the previous stage was inserted into one of the closed vessel. Then 37.5 ml of 1-butanol was added to the vessel. The addition of yellow solid and 1-butanol was repeated to fill up all the 6 closed vessels. These 6 vessels were then treated by microwave irradiation (1450 W) at 120 ℃ in a microwave digester for 4 hours.

After 4 hours treatment and about 20 minutes of cooling, the vessels were removed from the microwave digester. A blue solution with whitish-blue solid suspension was formed. The whitish-blue solid was then recovered using centrifuge technique and dried in oven for 48 hours. Whitish-blue solid precursor of vanadium hydrogen phosphate sesquihydrate ($VOHPO_4 \cdot 1.5H_2O$) was obtained.

The whole process to produce whitish-blue solid from yellow solid was then repeated for different microwave treatment durations, which are 5, 6 and 7 hours. Therefore, there are total 4 sets of whitish-blue solid of precursors were collected and proceeded to the calcination step to produce VPO catalysts.

+

6 × $VOPO_4 \cdot 2H_2O$ + 1-butanol

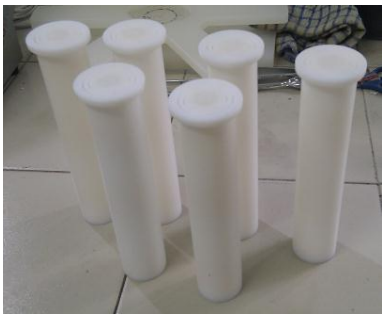

Closed Vessels

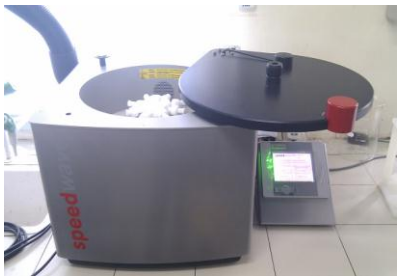

2nd Stage Microwave Treatment (1450 W): 4,5,6,7 hour 120 °C

Whitish-blue solid formed (wet)

Centrifugation

Normal Oven Drying: 48 hour 90 °C

2nd Stage Precursor $VOHPO_4 \cdot 1.5H_2O$ Dry whitish-blue solid

Figure 3.2: 2nd Stage of Microwave Treatment

3.2.3 Calcination

(Refer to Figure 3.3: Calcination)

The dried whitish-blue solid was sieved into fine powder and then calcined in a gas flow of 0.75 % of *n*-butane in air mixture at 460 ℃ for 18 hours. Dark green solid of VPO catalyst was formed. The VPO catalyst was then preceded to the analysis by some characterisation techniques.

The calcination process was repeated for 4 whitish-blue solid precursors with different microwave treatment durations. Therefore, there were total 4 sets of dark green solid of active VPO catalysts were collected, which were denoted as VPO-4, VPO-5, VPO-6 and VPO-7 according to their second stage microwave treatment durations. The catalysts were preceded to the analysis.

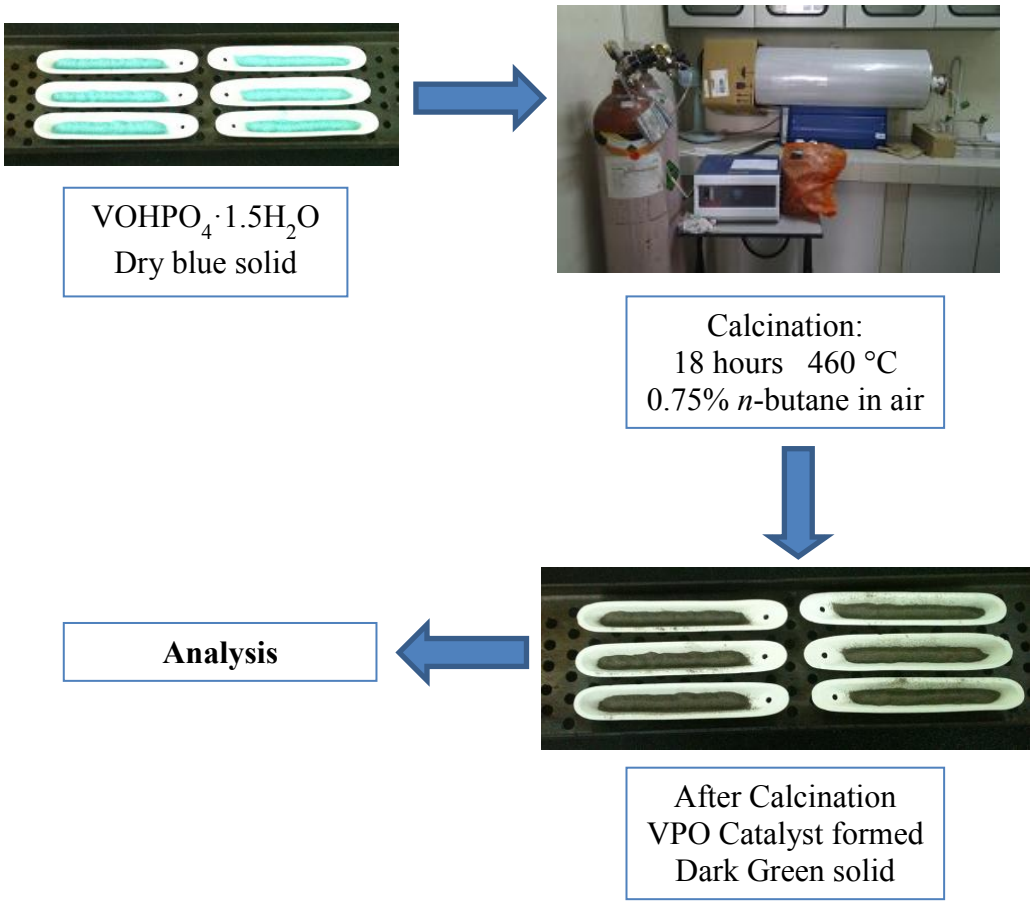

Figure 3.3: Calcination

3.3 Characterisation Techniques

Characterisation is an important field in catalysis to investigate the nature of an active catalyst. It helps to understand the synthesised catalyst better, so that improvement can be done. The ultimate goal of catalyst characterisation is to examine the physical and chemical properties under the reaction conditions, under which the catalyst operates. In industry, the emphasis is mainly on developing an active, selective, stable and mechanically robust catalyst (Chorkendorff & Niemantsverdriet, 2003).

To investigate the effect of different durations on the microwave treatment towards the physical and chemical properties of VPO catalysts synthesised, there are six characterisation techniques used. All the four VPO catalyst samples were analysed and compared using these techniques. X-rays Diffraction (XRD) analysis, Brunauer-Emmett-Teller (BET) and Scanning Electron Microscope (SEM) were used to examine the physical properties of the catalyst. Energy-Dispersive X-rays (EDX) analysis, Inductively Coupled Plasma-Optical Emission Spectroscopy (ICP-OES) and redox titration were used to study the chemical properties of the catalyst.

3.3.1 X-Rays Diffraction Analysis (XRD)

XRD is a common technique to analyse crystalline compounds in qualitative and quantitative way. The structural information of crystalline materials can be obtained relies on the dual wave or particle nature of X-rays. The penetrating radiation, X-rays was scattered when it enters a crystallite matter. A diffraction process occurs to have the scattered X-rays radiation undergo constructive and destructive interference. The intensity and the direction of the scattered X-rays radiation depend on the crystal lattice structure with respect to the incident beam.

XRD is used to identify crystalline phases inside catalysts by means of lattice structural parameters, and to obtain an indication of particle size. X-rays diffraction occurs in the elastic scattering of X-rays photons by atoms in a periodic lattice. The

scattered monochromatic X-rays that is in phase gives constructive interference (Chorkendorff & Niemantsverdriet, 2003).

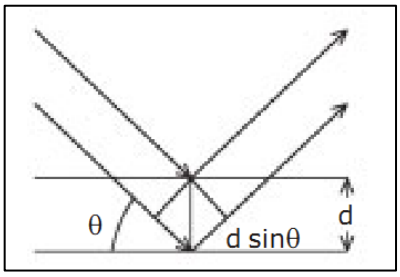

Figure 3.4: X-rays Diffraction Illustration

The Figure 3.4 above illustrates how diffraction of X-rays by crystal planes allows one to derive lattice spacings by using the Bragg's Law:

$$n\lambda = 2dsin\theta \quad ; \quad n = 1,2, \ldots \tag{3.1}$$

where

n = order of the reflection

λ = wavelength of the X-rays

d = distance between two lattice planes

θ = angle between the incoming X-rays and the normal to the reflecting lattice plane

One of the great advantages of using X-rays is their penetrating power. This enables XRD to monitor solid-state reactions such as reduction, oxidation and sulfidation in the activation of catalysts. The strength of XRD for catalyst characterisation is that it gives clear and unequivocal structure information on particles that are sufficiently large, along with an estimate of the size, and this information can be revealed under reaction conditions. However, there is a limitation for XRD that it cannot detect particles that are too small or amorphous (Chorkendorff & Niemantsverdriet, 2003).

The measurements were carried out using a Shimadzu diffractometer model XRD-6000 (Figure 3.5) to generate diffraction patterns from powder crystalline samples at ambient temperature. By employing Cu Kα radiation at 40 kV generated by Phillips glass diffraction X-rays tube broad focus 2.7 kW type on the catalyst that

were mounted on an aluminium sample holder. The basal spacing was determined via powder technique. The catalysts were scanned from $2\theta = 2\ °$ to $2\theta = 60\ °$. Each plane on crystalline solid has its own unique X-rays pattern at a specific angle of incident ray. The diffractogram (Graph of intensity against the scattering angle, 2θ) obtained were compared with the Joint Committee on Powder Diffraction Standards (JCPDS) PDF 1 database version 2.6 to confirm the catalytic phases. The phase composition and the crystallite sizes of VPO catalysts synthesised were then obtained.

Figure 3.5: Shimadzu LabX XRD-6000

3.3.2 Brunauer-Emmett-Teller (BET)

BET theory is a theory generalised of Langmuir's treatment of the unimolecular layer that explains the physical adsorption of gas molecule on a solid surface. BET is an important technique to analyse the specific surface area of a solid material (Brunauer, Emmett, & Teller, 1938).

The total surface areas of VPO catalysts were measured by nitrogen adsorption using a Sorptomatic BET from Thermo Fisher Scientific, which is shown in Figure 3.6. Besides, the Langmuir Isotherm of the VPO catalyst synthesised can be studied to obtain the sizes of the pores.

Figure 3.6: Thermo Sorptomatic BET

To obtain the specific surface area of the VPO catalysts, a tube was degassed first before taking its blank weight. Then, 0.5 g of VPO-4 catalyst was inserted to the tube and degassed again for one day before taking the actual sample weight. The degassed sample tube was then dipped into liquid nitrogen to undergo blank analysis using helium gas. The sample was again degassed for one day and dipped into liquid nitrogen to have sample analysis using nitrogen gas. The specific surface area of VPO-4 catalyst was then calculated by comparing the blank analysis and sample analysis. The procedures were repeated for VPO-5, VPO-6 and VPO-7 catalysts.

3.3.3 Scanning Electron Microscope (SEM)

Scanning electron microscope (SEM) is a straightforward technique to determine the size and shape of supported particle by employing a beam of electrons directed at the particle (Amelinckx, Dyck, Landurt, & Tendeloo, 1997). SEM involves rastering a narrow electron beam over the surface and detecting the yield of either secondary or backscattered electrons as a function of the position of the primary beam. The secondary electrons have mostly low energies and originate from the surface region of the sample. Backscattered electrons come from deeper and carry information on the composition of the sample (Chorkendorff & Niemantsverdriet, 2003).

The most widely used signal in the SEM is that from secondary electrons. Secondary electrons are detected by a scintillator-photomultiplier system known as the Everhart-Thornley detector. The secondary electrons strike a scintillator, which then emits light that transmitted into a photomultiplier which converts the photons into pulses of electrons. The pulses of electrons is then amplified and used to modulate the intensity of the cathode ray tube (CRT). The spot of the CRT is scanned across the screen to a television receiver, in a rectangular set of straight lines known as raster (Goodhew, Humphreys, & Beanland, 2001).

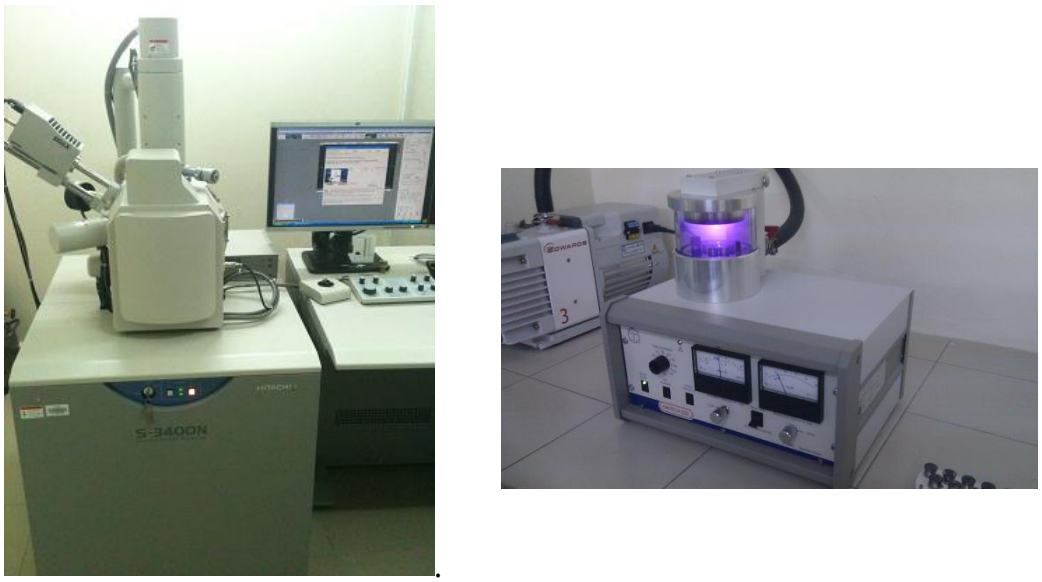

(a) **(b)**

Figure 3.7: (a) Hitachi VP-SEM S-3400N (b) Emitech Sputter Coater

The model of SEM used in this research is Hitachi VP-SEM S-3400N, which is shown in Figure 3.7(a). In this research, SEM is used to obtain the morphology and topology of the VPO catalyst synthesised. Morphology refers to the shape, size and arrangement of the particles making up object that are lying on the surface of the sample. Topography refers to the surface features of an object and its texture.

To obtain the micrograph of the VPO catalyst, little amount of the catalyst was placed in the sample container. The samples were then coated with gold using Emitech Sputter Coater (Figure 3.7b) before being analysed by SEM. The micrograph could be obtained by adjusting the magnification power that can clearly view the structure of the catalyst. The micrograph of that magnification was then captured and recorded.

3.3.4 Energy Dispersive X-ray Analysis (EDX)

Energy dispersive X-ray spectroscopy (EDX) is an important analysis technique to measure the elemental composition of a specimen. First, EDX focuses a high beam of X-rays into a specimen. Adsorption of X-ray photon leads to the ejection of a photoelectron from a lower energy inner shell and creating an electron space. Then an electron from outer higher energy shell will fill up the space. The energy difference between the lower energy inner shell and higher energy outer shell will be released a voltage signal that detected by an energy dispersive spectrometer. The data are then displayed as a histogram of intensity by voltage and further analysed for peak identification and quantification. This histogram allows the specimen elemental composition to be determined (Goldstein, et al., 2003).

The model of EDX instrument used in this research is Apollo-X EDX from Edax Ametex, which is attached to the SEM and shown in Figure 3.8. In this research, EDX was used to make an elemental analysis to make sure that there is only VPO catalyst without contaminant. Besides, the P/V ratio of the VPO catalyst can be calculated through this instrument. EDX analysis was carried out by EDAX software right after the SEM analysis.

Figure 3.8: Edax-Ametex Apollo-X EDX

First, little amount of the catalyst was placed in the sample container and coated with gold using Emitech Sputter Coater (Figure 3.7b) before being analysed by EDX. Similar to SEM, by adjusting the magnification power that can clearly view the site of the catalysts, the micrograph was captured and the elemental analysis graph was generated. Through the EDX analysis, phosphorus (P) and vanadium (V) contents on the surface of VPO catalysts were obtained. The P/V ratios were then calculated by dividing the P content with V content. The results from EDX were then compared to the P/V ratios results from ICP-OES.

3.3.5 Inductively Coupled Plasma Optical Emission Spectrometry (ICP-OES)

Inductively Coupled Plasma Optical Emission Spectrometry (ICP-OES) is an analytical technique used for detection of trace metals. Plasma is a hot, partially ionised gas that contains relatively high concentrations of ions and electrons. Plasma atomiser is often used as a power source for atomic emission, atomic fluorescence and atomic mass spectrometry. ICP is one of the power sources offering the greatest advantage in term of sensitivity and freedom from interference (Hill, 2006). Optical emission spectrometry (OES) is widely used in elemental analysis with inductively coupled plasma (ICP) as the power source.

The high temperature of the ICP is able to produce excited atoms and ions that emit electromagnetic radiation at wavelengths characteristic of a particular element (Stefansson, Gunnarsson, & Giroud, 2007). The radiation emitted is then

separated into its constituent wavelength by the wavelength isolation device. The light separated is then measured with a photomultiplier tubes as a direct reading spectrometers. The signals are then processed and provided as input to a computer system (Skoog, West, Holler, & Crouch, 2004).

The model of ICP-OES used in this research is Optima 7000 DV from PerkinElmer, which is shown in the Figure 3.9. In this research, IPC-OES functioned similar to EDX, which performs elemental analysis to the VPO catalyst, which is to make sure there is no contaminant in the catalyst. Besides, the P/V ratio of the VPO catalyst can be calculated since the proportion of phosphorous and vanadium can be obtained through this instrument.

The procedures to prepare sample solutions and standard solutions for both phosphorus and vanadium were included in Appendix A. The sample solutions were prepared to have concentration of 100 ppm, and three standard solutions were prepared with 10 ppm, 20 ppm and 40 ppm to have calibration graph. Through this analysis, the phosphorus (P) and vanadium (V) contents of the VPO catalysts were found. The P/V ratios were then calculated by dividing P content with V content.

Figure 3.9: PerkinElmer ICP-OES Optima 7000 DV

3.3.6 Redox Titration

Redox titration is a method developed by Niwa & Murakami (1982) to determine the mechanism of the ammoxidation of toluene, vanadium oxide supported on Al_2O_3. In this research, redox titration method was used to determine the average vanadium valence (*AV*) of the VPO catalyst. The method was separated and explained into three stages below:

In the first stage, a known amount of sample catalyst was dissolved in 100 ml of sulphuric acid (2 M of H_2SO_4) to form a greenish blue solution. After cooled to room temperature, the solution was titrated with potassium permanganate solution (0.01 N of $KMnO_4$) to oxidise the V^{3+} and V^{4+} in the solution to V^{5+}. The end point reached when the first drop of $KMnO_4$ that changed the colour of solution from greenish blue to pink. The volume of $KMnO_4$ used was recorded as V_1.

For second stage, the oxidised solution from the first stage was titrated with ammonium iron (II) sulphate solution (0.01 N) to reduce V^{5+} in the solution to V^{4+}. The indicator used was diphenylamine which showed violet colour in the oxidised solution. The end point reached when the first drop of ammonium iron (II) sulphate solution that decolourised the violet oxidised solution. The volume of ammonium iron (II) sulphate solution used was recorded as V_2.

Another fresh 25 ml of the original solution was then titrated with 0.01 N ammonium iron (II) sulphate solution. Diphenylamine is also used as indicator to have violet solution. This third stage of titration is to determine the V^{5+} in the original solution. The end point is reached when the first drop of ammonium iron (II) sulphate solution that changes the solution colour from violet to greenish blue. The volume of ammonium iron (II) sulphate solution used was recorded as V_3.

Before calculating the average vanadium valence (*AV*), the following equations were used to obtain the values for V^{3+}, V^{4+}, and V^{5+} values respectively (Niwa & Murakami, 1982):

$$V^{3+} = 20(0.01)V_1 - 20(0.01)V_2 + 20(0.01)V_3 \quad (3.2)$$

$$V^{4+} = 40(0.01)V_2 - 40(0.01)V_3 - 20(0.01)V_1 \quad (3.3)$$

$$V^{5+} = 20(0.01)V_3 \quad (3.4)$$

where

V_1 = volume of potassium permanganate used in first stage, cm^3

V_2 = volume of ammonium iron (II) sulphate used in second stage, cm^3

V_3 = volume of ammonium iron (II) sulphate used in third stage, cm^3

Finally, the average oxidation state of vanadium (AV) can be determined by the equation below:

$$AV = \frac{5V^{5+} + 4V^{4+} + 3V^{3+}}{(V^{5+} + V^{4+} + V^{3+})} \quad (3.5)$$

where

V^{3+} = concentration of vanadium at oxidation number of +3

V^{4+} = concentration of vanadium at oxidation number of +4

V^{5+} = concentration of vanadium at oxidation number of +5

CHAPTER 4

RESULTS AND DISCUSSION

4.1 Introduction

Vanadium phosphorus oxide (VPO) catalysts were prepared via sesquihydrate precursor ($VOHPO_4 \cdot 1.5H_2O$) method by microwave treatment method using microwave digester. VPO sesquihydrate precursors were prepared with a first stage microwave treatment of constant 1 hour, and proceeded with a second stage microwave treatment of variation of 4, 5, 6 and 7 hours. Normal drying method was applied to dry the precursors produced for both stages. The precursors obtained were then calcined with 0.75 % *n*-butane in air for 18 hours to produce VPO catalysts.

The catalysts obtained were denoted as VPO-4, VPO-5, VPO-6 and VPO-7 to represent their respective second stage microwave treatment durations. The effects of different second stage microwave treatment durations towards the physical and chemical properties of VPO catalysts were studied.

Table 4.1: Denotation of VPO Catalysts Synthesised

Catalyst	Second Stage Microwave Treatment Duration
VPO-4	4 hours
VPO-5	5 hours
VPO-6	6 hours
VPO-7	7 hours

4.2 X-rays Diffraction (XRD) Analysis

The XRD patterns of VPO-4, VPO-5, VPO-6 and VPO-7 are shown in Figure 4.1. According to result, four catalysts show similar diffraction patterns. There are three main characteristic peaks shown at 2θ = 22.9 °, 28.4 ° and 29.9 °, which correspond to (0 2 0), (2 0 4), and (2 2 1) reflection planes of VPO catalyst, respectively.

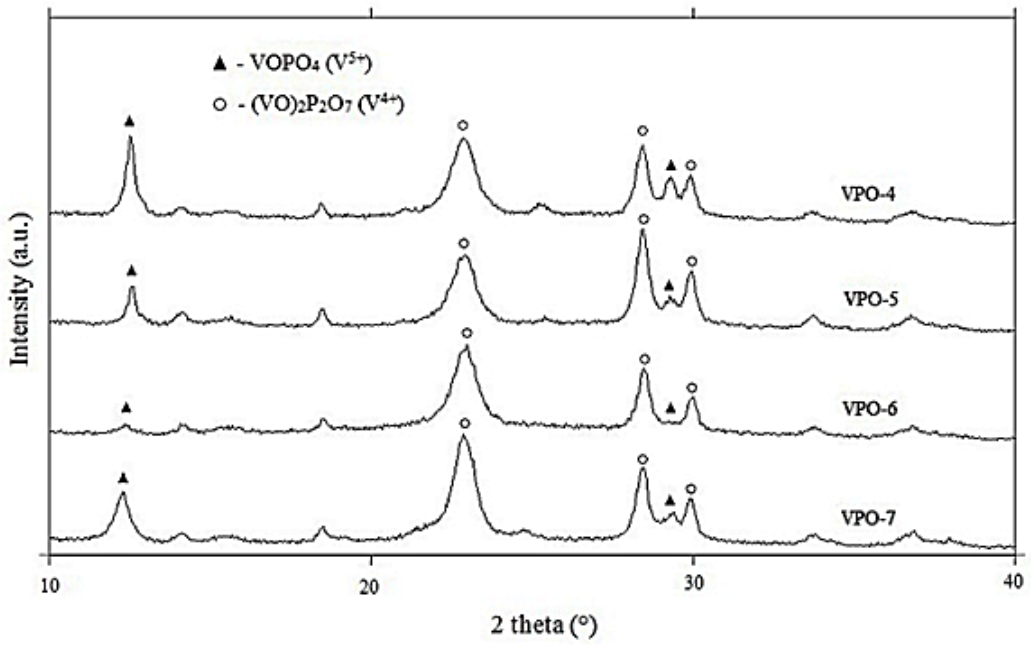

Figure 4.1: XRD Patterns for VPO Catalysts Synthesised

From the XRD patterns (Figure 4.1), only V^{4+} and V^{5+} phases appeared with no sign of V^{3+} phase. The peak of (0 2 0) phase (2θ = 22.9 °) was shown to be narrower and more intense as the second stage microwave treatment duration increased, indicating the increased of formation of V^{4+} phase.

An additional small peak emerged at 2θ = 29.3 ° were observed for VPO-4, VPO-5 and VPO-7, which indicates the existence of $VOPO_4$ (V^{5+}) phase. The intensity of this peak was found to be the most prominent for VPO-4 catalyst. Its intensity gradually decreased as the second stage microwave treatment duration increased from 4 to 6 hours, indicated that a longer microwave treatment durations would reduce the formation of V^{5+} phase in the catalyst. The small peak has totally disappeared for VPO-6, indicating that an amorphous type of V^{5+} phase could be

formed or the amount of this particular phase is below the detectable limit of the XRD instrument since the presence of V^{5+} phase could be detected in the redox titration techniques and will be discussed in the following section. When the precursor was further treated for a longer duration (i.e. 7 hours), the V^{5+} phase has been reformed. This could be rationalised that longer microwave treatment of more than 6 hours in the second stage would facilitate the formation of V^{5+} phase.

The crystallite size of (0 2 0) and (2 0 4) reflection planes for VPO-4, VPO-5, VPO-6 and VPO-7 were calculated by using the Debye-Scherrer equation (Klug & Alexander, 1974) below:

$$t(\text{Å}) = \frac{0.89\,\lambda}{\beta_{hkl} \times \cos\theta_{hkl}} \tag{4.1}$$

where,

t = crystallite size for (h k l) phase, Å

λ = X-rays wavelength of radiation for Cu Kα, Å

β_{hkl} = full width at half maximum (FWHM) at (h k l) peak, rad

θ_{hkl} = diffraction angle for (h k l) phase, °

The calculations of the crystallite sizes for all the VPO catalysts synthesised were shown in Appendix C and summarised in Table 4.2 below:

Table 4.2: XRD Data of VPO Catalysts Synthesised

Catalyst	Linewidth[a] (020)(°)	Linewidth[b] (204)(°)	Crystallite Size[c] (020)(Å)	Crystallite Size[c] (204)(Å)
VPO-4	0.9362	0.5701	85.58	142.09
VPO-5	0.9268	0.6209	86.45	130.47
VPO-6	0.9372	0.5810	85.49	139.44
VPO-7	0.8414	0.5647	95.22	143.45

[a] Full-width half maximum (FWHM) of (020) reflection plane

[b] Full-width half maximum (FWHM) of (204) reflection plane

[c] Crystallite size by means of Scherrer's formula

From the results of XRD in table 4.2, the crystallite sizes of four VPO catalysts were calculated to be almost the same. This has indicated that, different second stage microwave treatment durations do not significantly affect the crystallite sizes of the catalysts.

4.3 Brunauer-Emmett-Teller (BET) Surface Area Measurements

The specific surface area of the VPO catalysts synthesised were measured by BET using nitrogen adsorption method. The specific surface areas of the VPO catalysts synthesised are: 7.216 m^2/g for VPO-4, 15.553 m^2/g for VPO-5, 17.049 m^2/g for VPO-6 and 13.612 m^2/g for VPO-7 (Table 4.3).

Table 4.3: BET Surface Area of VPO Catalysts Synthesised

Catalysts	Specific Surface Area (m^2/g)
VPO-4	7.216
VPO-5	15.553
VPO-6	17.049
VPO-7	13.612

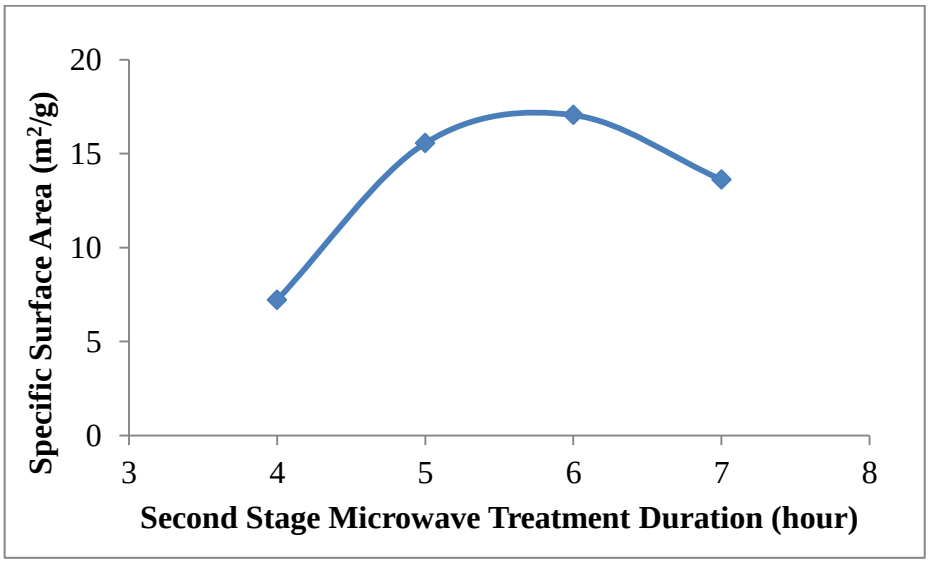

Figure 4.2: Graph of BET Specific Surface Area

These results from BET showed that an increase of second stage microwave treatment duration could increase the specific surface area of the VPO catalysts. Among all, 6 hours of second stage microwave treatment yielded the VPO catalyst with the highest specific surface area. However, the specific surface area decreased when the microwave treatment duration is more or less than 6 hours. This could be due to the forming of a more compact agglomeration of the VPO platelets as seen in the SEM micrographs. This particular phenomenon would cause the nitrogen gas atom to be no longer accessible to the surface of the catalysts and led to lower specific surface area.

Figures 4.3, 4.4, 4.5 and 4.6 were graphs showing the adsorption and desorption isotherm of the synthesised VPO catalysts. All the synthesised VPO catalysts have shown similar adsorption and desorption isotherm graphs, indicating that different second stage microwave treatment durations would not affect the type of isotherm of the catalyst. The isotherms graphs (Figure 4.3 – 4.6) showed that the VPO catalysts synthesised belongs to type IV isotherms. Type IV isotherm features a hysteresis loop characteristic generated by the capillary condensation taking place in mesopores (pores width between 2 nm to 50 nm) and the limiting uptake over a range of high relative pressure (IUPAC, 1982).

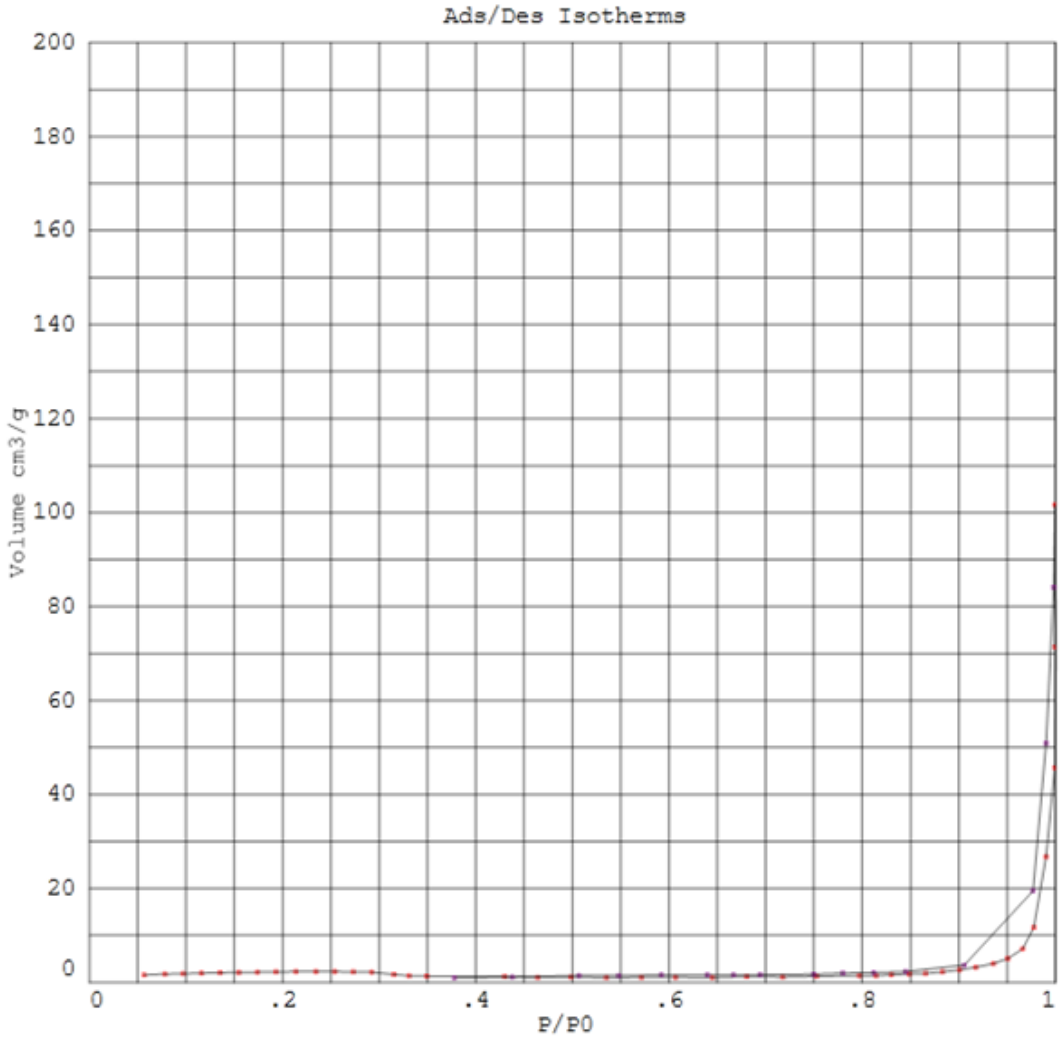

Figure 4.3: Adsorption/Desorption Isotherms for VPO-4

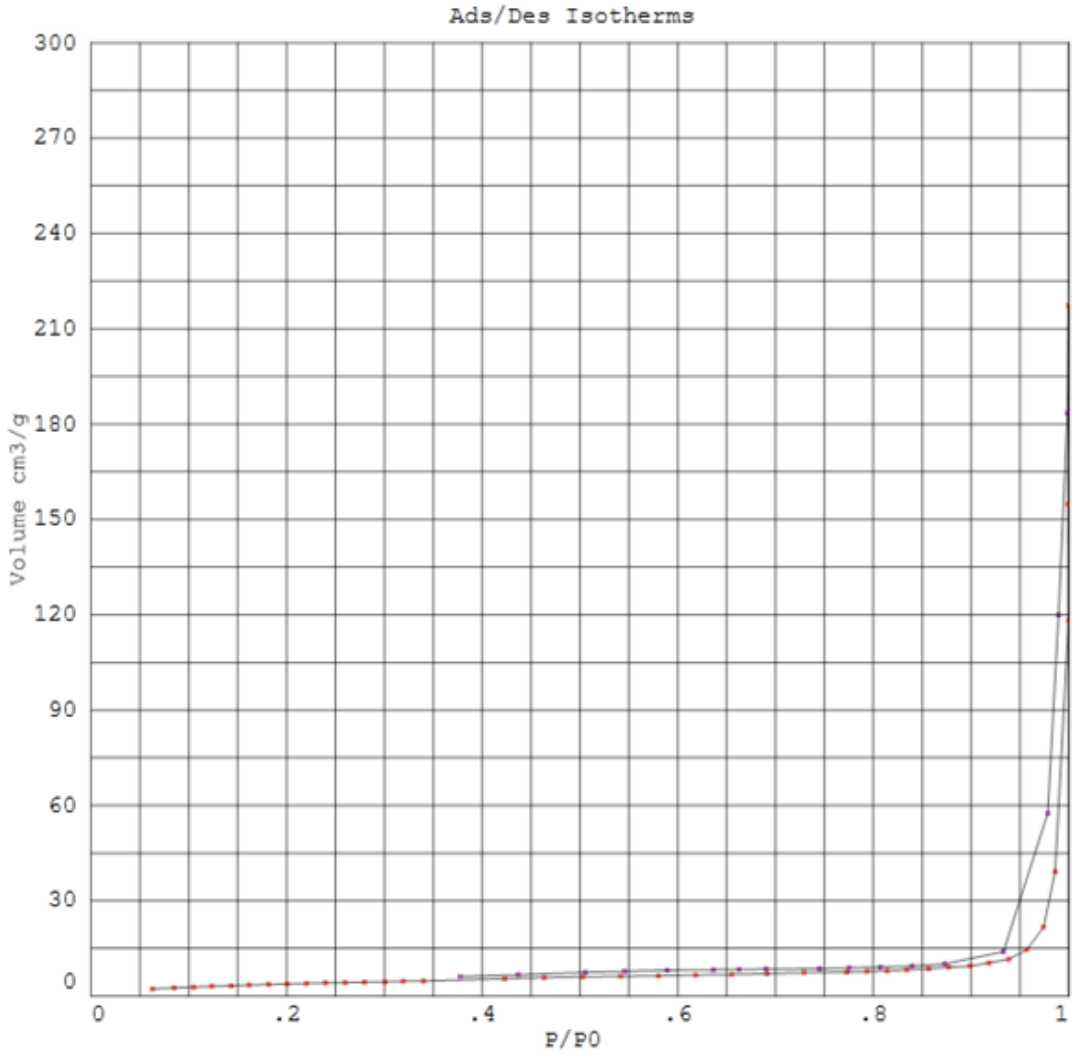

Figure 4.4: Adsorption/Desorption Isotherms for VPO-5

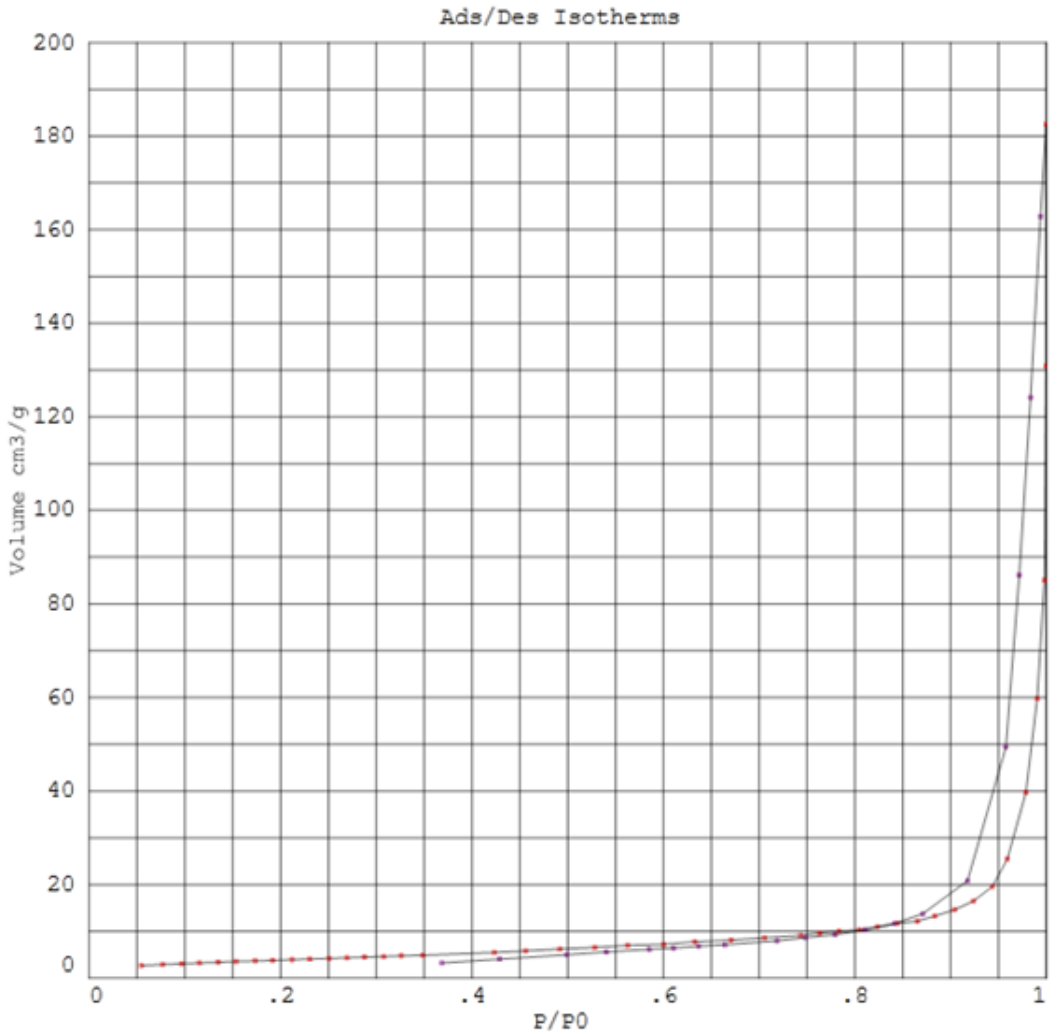

Figure 4.5: Adsorption/Desorption Isotherms for VPO-6

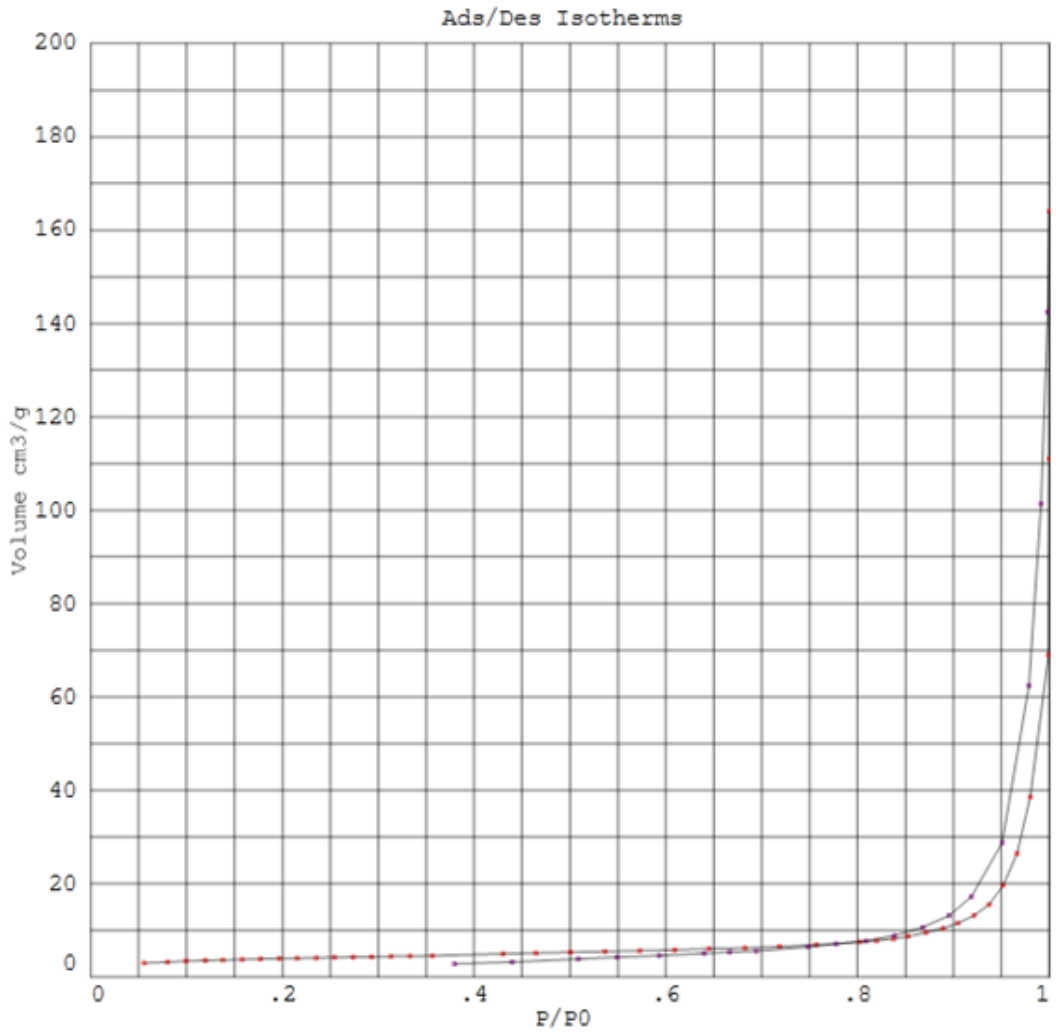

Figure 4.6: Adsorption/Desorption Isotherms for VPO-7

4.4 Scanning Electron Microscope (SEM)

The secondary electron micrographs on the surface of all the four catalysts undergone different second stage microwave treatment duration (4, 5, 6 and 7 hours) with low (×2000) and high (×10 000) magnifications were shown in Figures 4.7 to 4.10.

The catalysts synthesised showed agglomerated structure with the characteristic of rosette-shape clusters. These rosette shape clusters are actually composed of $(VO)_2P_2O_7$ crystallites that exposing the (1 0 0) plane (Kiely, Sajip, Ellison, Sananes, Hutchings, & Volta, 1995).

By comparing all of the micrographs, the formation of rosette-shape clusters could be observed in every VPO catalysts synthesised by microwave treatment. Therefore, different in second stage microwave treatment does not significantly affect the morphologies of the VPO catalysts.

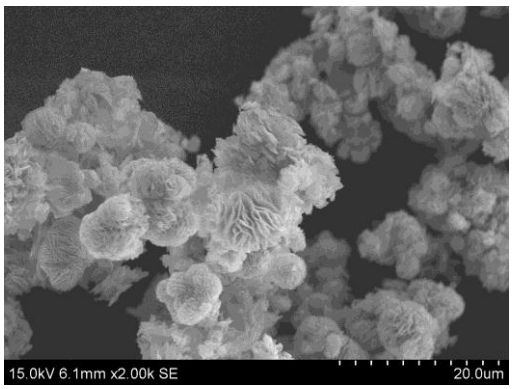

(a)

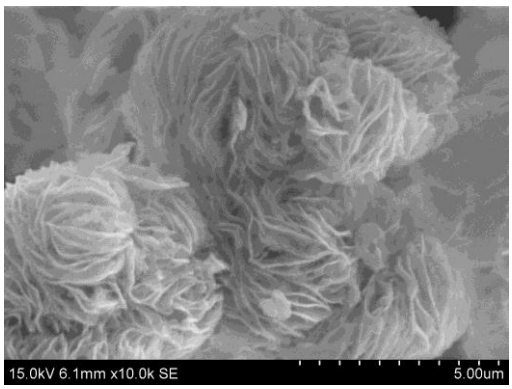

(b)

Figure 4.7: SEM Micrograph for VPO-4: (a) × 2000 and (b) × 10 000

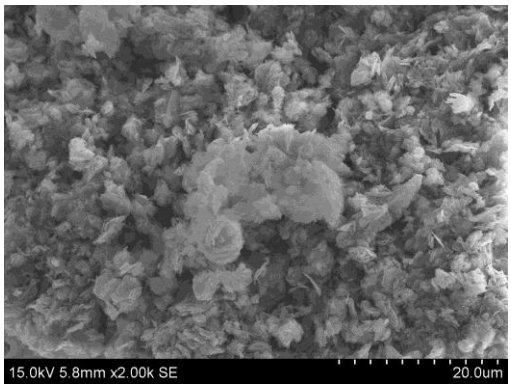

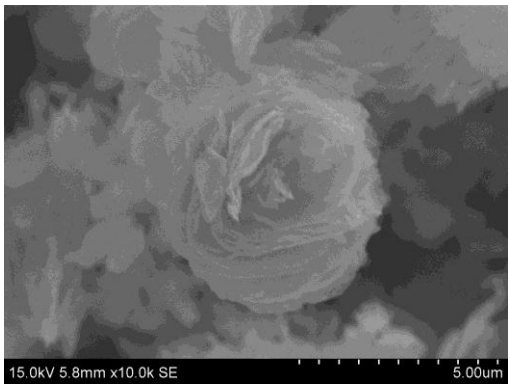

(a) **(b)**

Figure 4.8: SEM Micrograph for VPO-5: (a) × 2000 and (b) × 10 000

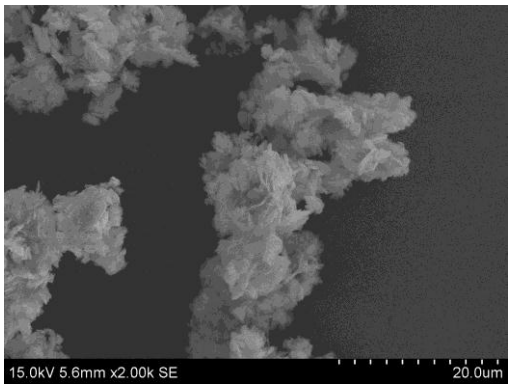

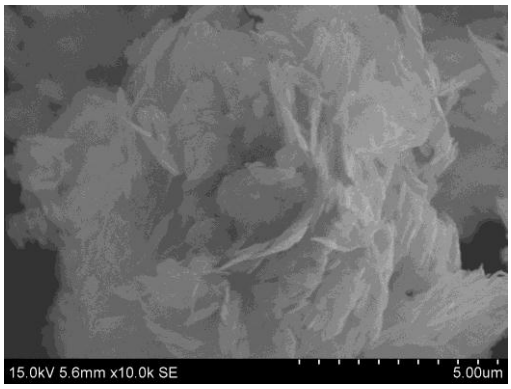

(a) **(b)**

Figure 4.9: SEM Micrograph for VPO-6: (a) × 2000 and (b) × 10 000

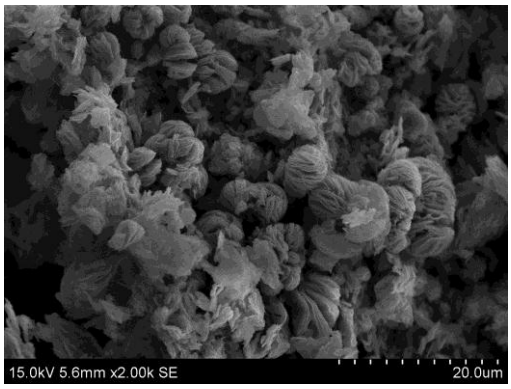

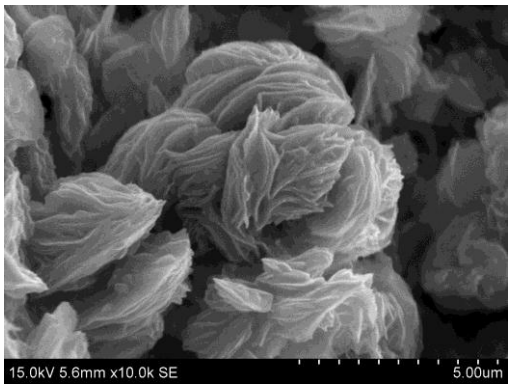

(a) **(b)**

Figure 4.10: SEM Micrograph for VPO-7: (a) × 2000 and (b) × 10 000

4.5 Energy Dispersive X-rays Analysis (EDX)

Due to inaccuracy of EDX, four different sites were selected to be analysed to reduce the errors, the average P/V ratio was then calculated and shown in table 4.4.

Table 4.4: EDX P/V Results

	Average P/V
VPO-4	**0.714**
VPO-5	**0.634**
VPO-6	**0.738**
VPO-7	**0.607**

The results above showed that the P/V ratio for all the four VPO catalysts synthesised are around 0.6 to 0.75. This is lesser than the optimum range of 1.0 to 1.2 (Spivey et al., 2005). There are two possible reasons for this outcome and the actual reason can only be concluded when these data were compared with the results from ICP-OES. The two possible reasons are:

1. Less phosphorus (P) was detected on the catalysts' surface
2. Microwave digester had inhibited the surface enrichment of phosphorus (P) on the VPO structure.

4.6 Inductively Coupled Plasma Optical Emission Spectrometry (ICP-OES)

By using the combination of ICP and OES, the concentrations of phosphorus (P) and vanadium (V) were found. The results of P/V atomic ratio for each VPO catalysts was calculated by dividing the concentration of P to the concentration of V. The results were shown in Table 4.5 below:

Table 4.5: ICP Results and Calculated P/V Ratio

Catalysts	Conc. of P (ppm)	Conc. of V (ppm)	**P/V ratio (ICP)**	P/V ratio (EDX)
VPO-4	22.74	28.16	**0.808**	0.714
VPO-5	20.82	26.63	**0.782**	0.634
VPO-6	22.45	23.63	**0.950**	0.738
VPO-7	21.99	29.62	**0.742**	0.607

From the results above (Table 4.5), the P/V ratios for all the VPO catalysts synthesised are between 0.742 and 0.950. The values obtained were relatively higher than the EDX results. However, P/V ratio obtained from ICP-OES is considered to be more reliable as it is a bulk analysis which could give a better understanding on the composition of the VPO catalysts.

It could be observed that, the P/V atomic ratio obtained via ICP-OES analysis was lower than unity due to the fact that the microwave treatment had inhibited the phosphorus (P) to be incorporated into the VPO structure. Among all the VPO catalysts synthesised, VPO-6 has the highest P/V ratio and close to 1. This had proven that the inhibition effect of phosphorus (P) to be incorporated into the VPO structure by microwave treatment was at the minimal if the second stage microwave treatment duration was set to six hours.

4.7 Redox Titration

By using the redox titration method developed by Niwa & Murakami (1982), the concentrations of V^{4+} and V^{5+} phase were calculated. The average oxidation numbers of vanadium, V_{AV} were then calculated. The titration results and calculations involved were shown in Appendix D.

Table 4.6: Average Oxidation Numbers of Vanadium

Catalysts	V^{4+} (%)	V^{5+} (%)	V_{AV}
VPO-4	79.49	20.51	4.2051
VPO-5	84.77	15.23	4.1523
VPO-6	80.95	19.05	4.1905
VPO-7	76.71	23.29	4.2329

From redox titration analyses, the calculated average vanadium valences (V_{AV}) for VPO-4, VPO-5, VPO-6 and VPO-7 are 4.2051, 4.1523, 4.1905 and 4.2329 respectively. The redox titration results obtained shows that the average oxidation number of vanadium (V_{AV}) was slightly higher than 4.0 which had indicated that all the catalysts produced do consist of both V^{4+} and V^{5+} phases. V^{4+} phase (i.e. $(VO)_2P_2O_7$) was shown to be the dominant phase and only a small fraction of the catalysts belong to the V^{5+} phase (i.e. $VOPO_4$). The obtained results were well-agreed with the XRD patterns (Figure 4.1) as discussed in the earlier discussion part.

CHAPTER 5

CONCLUSION AND RECOMMENDATIONS

5.1 Conclusion

The catalysts obtained were denoted as VPO-4, VPO-5, VPO-6 and VPO-7 to represent their respective second stage microwave treatment durations. The effects of different second stage microwave treatment durations towards the physical and chemical properties of VPO catalysts were studied.

As a summary, VPO-6 has exhibited the highest specific surface area as observed in BET and P/V atomic ratio closest to one as observed in EDX and ICP-OES. VPO-5 has the lowest average vanadium valence (V_{AV}) as calculated in redox titration. Generally, all the synthesised catalysts exhibit similar crystallite sizes and surface morphologies as seen in XRD and SEM, respectively.

Therefore, VPO-6 which went through 6 hours second stage microwave treatment was chosen as the best catalysts out of the four catalysts synthesised. This is due to its highest specific surface area and the best P/V atomic ratio if compared to the other three synthesised catalysts.

In conclusion,

1. VPO catalysts were successfully synthesised through microwave treatment and normal drying method.
2. Different second stage microwave treatment durations do not markedly affect the crystallite sizes, surface morphologies of the VPO catalysts synthesised.
3. 6 hours of second stage microwave treatment could synthesise the best compromise of VPO catalysts. Treatment durations of more or less than 6 hours would decrease the specific surface area and P/V atomic ratio of VPO catalyst.

5.2 Recommendations

For further research,

1. Phosphorus (P) content must be increased by increasing the amount of *o*-phosphoric acid used so that the P/V ratios can be controlled to be 1 to 1.2 to have better VPO performance.
2. The second stage microwave treatment can be set to be constantly 6 hours, but varies the first stage microwave treatment to study the effect of first stage microwave treatment towards physical and chemical properties of VPO.
3. Various dopants can be added so that the effect of microwave treatment method towards the physical, chemical, reactivity and catalytic properties of doped VPO catalysts can be studied.

REFERENCES

Abon, M., & Volta, J. (1997). Vanadium phosphorus oxides for n-butane oxidation to maleic anhydride. *Applied Catalysis A: General, 157* (1-2), 173-193.

Amelinckx, S., Dyck, D. V., Landurt, J. V., & Tendeloo, G. V. (1997). *Handbook of Microscopy.* Weinheim: Wiley-VCH.

Bergeret, G., David, M., Broyer, J., & Volta, J. (1987). A contribution to the knowledge of the active sites of VPO catalysts for butane oxidation to maleic anhydride. *Catalysis Today, 1* (1-2), 37-47.

Bergman, R., & Frisch, N. (1966). *Patent No. 3 293 268.* US.

Berry, F. J., Smart, L. E., Prasad, P. S., Lingaiah, N., & Rao, P. K. (2000). Microwave heating during catalyst preparation: influence on the hydrodechlorination activity of alumina-supported palladium-iron bimetallic catalysts. *Applied Catalysis A: General, 204* (2), 191-201.

Bordes, E., & Courtine, P. (1979). Some selectivity criteria in mild oxidation catalysis: VPO phases in butene oxidation to maleic anhydride. *Journal of Catalysis, 57* (2), 236-252.

Boreskov, G. (2003). *Heterogeneous Catalysis.* New York: Nova Science Publlishers, Inc.

Brunauer, S., Emmett, P. H., & Teller, E. (1938). Adsorption of gases in multimolecular layers. *Journal of the American Chemical Society, 60* (1), 309-319.

Busca, G., Centi, G., & Trifiro, F. (1987). *Catalyst Deactivation 1987: proceedings of the 4th international symposium, Antwerp*. New York: Elsevier Science Publishers B. V.

Cavani, F., & Trifiro, F. (1994). Catalysing butane oxidation to make maleic anhydride. *ChemInform, 25* (34), 18-25.

Centi, G. (1993). Vanadyl Pyrophosphate - A Critical Overview. *Catalysis Today, 16* (1), 5-26.

Centi, G., Cavani, F., & Trifiro, F. (2001). *Selective oxidation by heterogeneous catalysis.* New York: Kluwer Academic / Plenum Publishers.

Chorkendorff, I., & Niemantsverdriet, J. (2003). *Concepts of Modern Catalysis and Kinetics.* Weinheim: Wiley-VCH.

Cornaglia, L., C.Caspani, & Lombardo, E. (1991). Physicochemical characterisation and catalytic behaviour of VPO formulations. *Applied Catalysis*, *74* (1), 15-27.

Ertl, G., & Freund, H. (1999). Catalysis and surface science. *Physics Today, 52* (1), 32.

Felthouse, T., Burnett, J., Horrell, B., Mummey, M., & Kuo, Y. (2001). *Maleic anhydride, maleic acid and fumaric acid*. Retrieved April 18, 2011, from http://www.usouthal.edu/chemistry/barletta/felthouse.pdf.

Fogler, H. (2006). *Elements of chemical reaction engineering* (4th ed.). Asia: Pearson Education, Inc.

Goldstein, J., Newbury, D., Joy, D., Lyman, C., Echlin, P., Lifshin, E., et al. (2003). *Scanning electron microscope and x-ray microanalysis* (3rd ed.). Springer.

Goodhew, P., Humphreys, F., & Beanland, R. (2001). *Electron Microscopy and Analysis* (3rd ed.). London: Taylor & Francis.

Haber, J. (2009). Fifty years of my romanace with vanadium oxide catalysts. *Catalysis Today, 142* (3-4), 100-113.

Hartley, F. (1985). *Supported metal complexes: a new generation of catalysts.* United States: D. Reidel Publishing Company.

Hill, S. J. (2006). *Inductively Coupled Plasma Spectrometry and Its Applications (2nd ed.).* Boca Raton, FL: Backwell Publishing Ltd.

Hutchings, G. J., Sananes, M. T., Sajip, S., Kiely, C. J., Burrows, A., Ellison, I. J., et al. (1997). Improved method of preparation of vanadium phosphate catalysts. *Catalysis Today, 33* (1-3), 161-171.

Ishimura, T., Sugiyama, S., & Hayashi, H. (2000). Vanadyl hydrogenphosphate sesquihydrate as a precursor for preparation of (VO)2P2O7 and cobalt-incorporated catalysts. *Journal of Molecular Catalysis A: Chemical, 158* (2), 559-565.

IUPAC (1982). Reporting physisorption data for gas/solid systems with special reference to the determination of surface area and porosity. *Pure & Appl. Chem., 54* (11), 2201-2218.

Janjic, N., & Scurrell, M. S. (2002). Evidence for the enhancement of the catalytic action of Zn-ZSM-5-based catalysts for propane aromatization using microwave radiation. *Catalysis Communications, 3* (6) , 253-256.

Kiely, C. J., Sajip, S., Ellison, I. J., Sananes, M. T., Hutchings, G. J., & Volta, J.-C. (1995). Electron microscopy studies of vanadium phosphorus oxide catalysts derived from vanadyl dihydrate. *Catalysis Letters, 33*, 357-368.

Klug, P. H., & Alexander, L. E. (1974). *X-ray diffraction procudures for polycrystalline and amorphous materials.* New York: John Wiley and Sons.

Kroschwitz, J., & Howe-Grant, M. (1991). *Encyclopedia of Chemical Technology.* New York: Wiley.

Kuo, P., & Yang, B. (1989). AlPO4 as a support material for VPO catalysts. *Journal of Catalysis, 117* (2), 301-310.

Matar, S., & Hatch, L. (2000). *Chemistry of Petrochemical Processes (2nd ed.).* United States of America: Gulf Publishing Company.

Moser, T., Wenig, R., & Schrader, G. (1987). Maleic anhydride conversion by VPO catalysts. *Applied Catalysis, 34*, 39-48.

Niwa, M., & Murakami, Y. (1982). Reaction mechanism of ammoxidation of toluene: IV. Oxidation state of vanadium oxide and its reactivity for toluene oxidation. *Journal of Catalysis, 76* (1), 9-16.

Ramstetter, A., & Baerns, M. (1988). Infrared spectroscopic investigation of the adsorption states of 1-butene, 1,3-butadiene, furan, 2,5H-furanone, and maleic anhydride on alumina-supported V2O5-P2O5 catalyst: I. Adsorption under nonreactive conditions. *Journal of Catalysis, 109* (2), 303-313.

Rothenberg, G. (2008). *Catalysis: Concepts and green applications.* Weinheim: Wiley.

Ruiz, P., & Delmon, B. (1992). *New Developments in selective oxidation by heterogeneous catalysis.* Belgium: Elsevier.

Sadiq, M., M.Bensitel, Nohair, K., Leglise, J., & Lamonier, C. (2011). Effect of calcination temperature on the structure of vanadium phosphorus oxide materials and their catalytic activity in the decomposition of 2-propanol. *Journal of Saudi Chemical Society*.

Shima, K., & Hatano, M. (1997). Maleic anhydride by heterogeneous oxidation of n-butane. *Applied Surface Science, 121-122*, 452-460.

Skoog, D., West, D., Holler, F., & Crouch, S. (2004). *Fundamentals of Analytical Chemistry 8th Edition.* International: Brooks/Cole Thomson Learning, Inc.

Spivey, J., Guliants, V., & Carreon, M. (2005). Vanadium-phosphorus-oxides: From fundamentals of n-butane oxidation to synthesis of new phases. In *Catalysis* (p. 1-45). UK: RSC Publishing.

Stefansson, A., Gunnarsson, I., & Giroud, N. (2007). New methods for the direct determination of dissolved inorganic, organic and total carbon in natural waters by Reagent-Free Ion Chromatography and inductively coupled plasma atomic emission spectrometry. *Analytica Chimica Acta, 582* (1), 69-74.

Taufiq-Yap, Y. H., Leong, L. K., Hussien, M. Z., Irmawati, R., & Hamid, S. B. (2004). Synthesis and characterisation of vanadyl pyrophosphate catalysts via vanadyl hydrogen phosphate sesquihydrate precursor. *Catalysis Today, 93-95*, 715-722.

Wang, W.-H. C. (1997). Effect of calcination environment on the selective oxidation of n-butane to maleic anhydride over promoted and unpromoted VPO catalysts. *Applied Catalysis A: General, 156* (1), 57-69.

Y.H. Taufiq-Yap, C. S. (2008). Effect of different calcination environments on the vanadium phosphate catalysts for selective oxidation of propane and n-butane. *Catalysis Today, 131* (1-4), 285-291.

Y.H. Taufiq-Yap, M. L. (2001). The Effect of The Duration of n-butane/air Pretreatment on The Morphology and Reactivity of (VO)2P2O7 Catalysts. *Catalysis Letters, 74* (1-2), 99-104.

Zeng, L., Jiang, H., & Niu, J. (2005). The study of L-VPO catalysts prepared by microwave treatment. *Journal of Molecular Catalysis A: Chemical, 232* (1-2), 119-122.

APPENDICES

APPENDIX A: ICP Preparation

1. Prepare 500 ml of 8M HNO_3

Concentrated HNO_3 available → 70 % purity, 1.42 g/cm^3 density

$$Molarity\ of\ HNO_3 = \frac{Density\ of\ HNO_3}{MW\ of\ HNO_3} \times purity \times 1000$$

$$= \frac{1.42\ g/cm^3}{63.01\ g/mol} \times 0.70 \times 1000$$

$$= 15.78\ M$$

By using the solution preparation equation,

$$m_1V_1 = m_2V_2$$

$$(15.78\ M)(V_1) = (8\ M)(500\ ml)$$

$$V_1 = 253.56\ ml$$

Therefore, procedures to obtain 500 ml of 8 M HNO_3 are:

(i) Measure **253.56 ml** of HNO_3

(ii) Top up to 500 ml bottle with deionized water

2. **Prepare V standard solution**
   (i) Weigh **0.1148 g** of NH_4VO_3
   (ii) Dissolve in a small beaker of deionized water (heat and stir)
   (iii) Top up to 1 L bottle (V stock solution) with deionized water (50 ppm now)
   (iv) V standard solution:
   10 ppm: 20 ml V stock solution + 10 ml 8M HNO_3 → top up to 100 ml
   20 ppm: 40 ml V stock solution + 10 ml 8M HNO_3 → top up to 100 ml
   40 ppm: 80 ml V stock solution + 10 ml 8M HNO_3 → top up to 100 ml

3. **Prepare P standard solution**
   (i) Weigh **0.1857 g** of $NH_4H_2PO_4$
   (ii) Dissolve in a small beaker of deionized water (heat and stir)
   (iii) Top up to 1 L bottle (P stock solution) with deionized water (50 ppm now)
   (iv) P standard solution:
   10 ppm: 20 ml P stock solution + 10 ml 8M HNO_3 → top up to 100 ml
   20 ppm: 40 ml P stock solution + 10 ml 8M HNO_3 → top up to 100 ml
   40 ppm: 80 ml P stock solution + 10 ml 8M HNO_3 → top up to 100 ml

4. **Sample Preparation**
   (i) Weigh **0.01 g** of sample in a small beaker
   (ii) Add 10 ml 8M HNO_3 (heat and stir)
   (iii) Top up to 100 ml bottle (100 ppm)

5. **Prepare Blank Solution**
   (i) Measure 10 ml of HNO_3 → top up to 100 ml

APPENDIX B: Redox Titration Preparation

1. Prepare 1000 ml of 2 M H_2SO_4 solution

Concentrated H_2SO_4 available → 95-98 % purity, 1.84 g/cm^3 density

$$Molarity\ of\ H_2SO_4 = \frac{Density\ of\ H_2SO_4}{MW\ of\ H_2SO_4} \times purity \times 1000$$

$$= \frac{1.84\ g/cm^3}{98.07\ g/mol} \times 0.95 \times 1000$$

$$= 17.82\ M$$

By using the solution preparation equation,

$$m_1V_1 = m_2V_2$$

$$(17.82\ M)(V_1) = (2\ M)(1000\ ml)$$

$$V_1 = 112.23\ ml$$

Therefore, procedures to obtain 1000 ml of 2 M H_2SO_4 are:

(i) **112.23 ml** of H_2SO_4 was measured

(ii) H_2SO_4 was transferred and topped up to 1000 ml with deionized water

2. Prepare 1000 ml of 0.1 M H_2SO_4

By using the solution preparation equation,

$$m_1V_1 = m_2V_2$$
$$(17.82\ M)(V_1) = (0.1\ M)(1000\ ml)$$
$$V_1 = 5.61\ ml$$

Therefore, procedures to obtain 1000 ml of 0.1 M H_2SO_4 are:

(i) **5.61 ml** of H_2SO_4 was measured

(ii) H_2SO_4 was transferred and topped up to 1000 ml with deionized water

3. Prepare 1000 ml of 0.01 N potassium permanganate, $KMnO_4$

Normality, N (eq/L) = M (mol/L) x *n* (eq/mol)

From the equation: $MnO^{4-} + 8\ H^{+} + 5e^{-} \leftrightarrow Mn^{2+} + 4\ H_2O$

$$\text{Molarity, M (mol/L)} = \frac{\text{N (eq/L)}}{n\ \text{(eq/mol)}}$$
$$= \frac{0.01}{5}$$
$$= 0.002\ \text{M}$$

MW of $KMnO_4$ = 158.04 g/mol

Weight for $KMnO_4$ in 1000 cm^3 H_2SO_4 (0.1 M) = 0.002 x 158.04

= 0.3161 g

Therefore, procedures to obtain 1000 ml of 0.01 N $KMnO_4$ are:

(i) **0.3161 g** of $KMnO_4$ was measured

(ii) $KMnO_4$ was dissolved in 1000 ml H_2SO_4 (0.1 M)

4. Prepare 1000 ml of 0.01 N ammonium iron (II) sulphate, $(NH_4)_2Fe(SO_4)_2 \cdot 6H_2O$

Normality, N (eq/L) = M (mol/L) x *n* (eq/mol)

From the equation: $Fe^{2+} + e^- \leftrightarrow Fe^{3+}$

$$\text{Molarity, M (mol/L)} = \frac{\text{N (eq/L)}}{n\,\text{(eq/mol)}}$$

$$= \frac{0.01}{1}$$

$$= 0.01\,\text{M}$$

MW of $(NH_4)_2Fe(SO_4)_2 \cdot 6H_2O$ = 391.99 g/mol

Weight for $(NH_4)_2Fe(SO_4)_2 \cdot 6H_2O$ in 1000 cm^3 H_2SO_4 (0.1 M)

= 0.01 x 391.99

= 3.9199 g

Therefore, procedures to obtain 1000 ml of 0.01 N $(NH_4)_2Fe(SO_4)_2 \cdot 6H_2O$ are:

(i) **3.9199 g** of $(NH_4)_2Fe(SO_4)_2 \cdot 6H_2O$ was measured

(ii) $(NH_4)_2Fe(SO_4)_2 \cdot 6H_2O$ was dissolved in 1000 ml H_2SO_4 (0.1 M)

5. Preparation of Diphenylamine, Ph_2NH, indicator

1 g of diphenylamine was weighed and dissolved in a few ml of concentrated sulphuric acid, H_2SO_4. Then the solution was transferred to a 100 ml volumetric flask and further top up with concentrated H_2SO_4.

APPENDIX C: XRD Crystallite Size Calculations

The crystallite sizes of catalysts were calculated by using the Debye-Scherrer equation (Klug & Alexander, 1974) below:

$$t(\text{Å}) = \frac{0.89\,\lambda}{\beta_{hkl} \times cos\,\theta_{hkl}}$$

where,

t = crystallite size for ($h\ k\ l$) phase, Å

λ = X-rays wavelength of radiation for Cu Kα, 1.54 Å

β_{hkl} = full width at half maximum (FWHM) at ($h\ k\ l$) peak, rad

θ_{hkl} = diffraction angle for ($h\ k\ l$) phase, °

VPO-4

3 strongest peaks from XRD analysis:

Peak no	2θ (°)	θ (°)	FWHM (°)	FWHM (rad)
6	22.8409	11.4205	0.9362	0.01634
9	28.4002	14.2001	0.5701	0.00995
11	29.8800	14.9400	0.5258	0.00918

For peak number 6 (2θ = 22.8409 °), which corresponds to (0 2 0) plane,

$$t(\text{Å}) = \frac{0.89 \times 1.54}{0.01634 \times cos\ 11.4205\,°} = \mathbf{85.58}\ \text{Å}$$

For peak number 9 (2θ = 28.4002 °), which corresponds to (2 0 4) plane,

$$t(\text{Å}) = \frac{0.89 \times 1.54}{0.00995 \times cos\ 14.2001\,°} = \mathbf{142.09}\ \text{Å}$$

VPO-5

3 strongest peaks from XRD analysis:

Peak no	2θ (°)	θ (°)	FWHM (°)	FWHM (rad)
6	22.8518	11.4259	0.9268	0.01618
10	28.4124	14.2062	0.6209	0.01084
12	29.8800	14.9400	0.636	0.01110

For peak number 6 (2θ = 22.8518 °), which corresponds to (0 2 0) plane,

$$t(\text{Å}) = \frac{0.89 \times 1.54}{0.01618 \times cos\ 11.4259\,^{\circ}} = \mathbf{86.45}\ \text{Å}$$

For peak number 10 (2θ = 28.4124 °), which corresponds to (2 0 4) plane,

$$t(\text{Å}) = \frac{0.89 \times 1.54}{0.01084 \times cos\ 14.2062\,^{\circ}} = \mathbf{130.47}\ \text{Å}$$

VPO-6

3 strongest peaks from XRD analysis:

Peak no	2θ (°)	θ (°)	FWHM (°)	FWHM (rad)
7	22.8923	11.4462	0.9372	0.01636
10	28.4498	14.2249	0.581	0.01014
11	29.9321	14.9661	0.5597	0.00977

For peak number 7 (2θ = 22.8923 °), which corresponds to (0 2 0) plane,

$$t(\text{Å}) = \frac{0.89 \times 1.54}{0.01636 \times cos\ 11.4462\,^{\circ}} = \mathbf{85.49}\ \text{Å}$$

For peak number 10 (2θ = 28.4498 °), which corresponds to (2 0 4) plane,

$$t(\text{Å}) = \frac{0.89 \times 1.54}{0.01014 \times cos\ 14.2249\,^{\circ}} = \mathbf{139.44}\ \text{Å}$$

VPO-7

3 strongest peaks from XRD analysis:

Peak no	2θ (°)	θ (°)	FWHM (°)	FWHM (rad)
7	22.8723	11.4362	0.8414	0.01469
9	28.4079	14.2040	0.5647	0.00986
11	29.8800	14.9400	0.5344	0.00933

For peak number 7 (2θ = 22.8723 °), which corresponds to (0 2 0) plane,

$$t(\text{Å}) = \frac{0.89 \times 1.54}{0.01469 \times cos\ 11.4362\,^\circ} = \mathbf{95.22}\ \text{Å}$$

For peak number 9 (2θ = 28.4079 °), which corresponds to (2 0 4) plane,

$$t(\text{Å}) = \frac{0.89 \times 1.54}{0.00986 \times cos\ 14.2040\,^\circ} = \mathbf{143.45}\ \text{Å}$$

APPENDIX D: Redox Titration Calculations

To get better result, the redox titration was repeated for 2 times, and the average reading was the calculated.

VPO-4	1st Reading	2nd Reading	Average
V_1	6.5	6.7	6.6
V_2	8.1	7.9	8
V_3	1.7	1.5	1.6

VPO-5	1st Reading	2nd Reading	Average
V_1	8.5	8.7	8.6
V_2	8.5	8.8	8.65
V_3	1.2	1.1	1.15

VPO-6	1st Reading	2nd Reading	Average
V_1	8.3	8.6	8.45
V_2	8.9	8.3	8.6
V_3	1.5	1.3	1.4

VPO-7	1st Reading	2nd Reading	Average
V_1	7.4	7.2	7.3
V_2	8.2	8.1	8.15
V_3	1.5	1.9	1.7

According to Niwa & Murakami, 1982, the following equations were used to obtain the concentration of vanadium at different oxidation state:

$V^{3+} = 20(0.01)V_1 - 20(0.01)V_2 + 20(0.01)V_3$

$V^{4+} = 40(0.01)V_2 - 40(0.01)V_3 - 20(0.01)V_1$

$V^{5+} = 20(0.01)V_3$

Finally, the average oxidation state of vanadium (*AV*) can be determined by the equation below:

$$AV = \frac{5V^{5+} + 4V^{4+} + 3V^{3+}}{(V^{5+} + V^{4+} + V^{3+})}$$

However, there is no formation of V^{3+} phase shown in XRD analysis. Therefore, the equation was reduced to:

$$AV = \frac{5V^{5+} + 4V^{4+}}{(V^{5+} + V^{4+})}$$

For VPO-4,

From experiment, $V_1 = 6.6$, $V_2 = 8$, $V_3 = 1.6$

$V^{4+} = 40(0.01)(8) - 40(0.01)(1.6) - 20(0.01)(6.6) = 1.24$

$V^{5+} = 20(0.01)(1.6) = 0.32$

$$AV = \frac{5(0.32) + 4(1.24)}{(0.32 + 1.24)} = \mathbf{4.2051}$$

For VPO-5,

From experiment, $V_1 = 8.6$, $V_2 = 8.65$, $V_3 = 1.15$

$V^{4+} = 40(0.01)(8.65) - 40(0.01)(1.15) - 20(0.01)(8.6) = 1.28$
$V^{5+} = 20(0.01)(1.15) = 0.23$

$$AV = \frac{5(0.23) + 4(1.28)}{(0.23 + 1.28)} = \mathbf{4.1523}$$

For VPO-6,

From experiment, $V_1 = 8.45$, $V_2 = 8.6$, $V_3 = 1.4$

$V^{4+} = 40(0.01)(8.6) - 40(0.01)(1.4) - 20(0.01)(8.45) = 1.19$
$V^{5+} = 20(0.01)(1.4) = 0.28$

$$AV = \frac{5(0.28) + 4(1.19)}{(0.28 + 1.19)} = \mathbf{4.1905}$$

For VPO-7,

From experiment, $V_1 = 6.6$, $V_2 = 8$, $V_3 = 1.6$

$V^{4+} = 40(0.01)(8) - 40(0.01)(1.6) - 20(0.01)(6.6) = 1.12$
$V^{5+} = 20(0.01)(1.6) = 0.34$

$$AV = \frac{5(0.34) + 4(1.12)}{(0.34 + 1.12)} = \mathbf{4.2329}$$